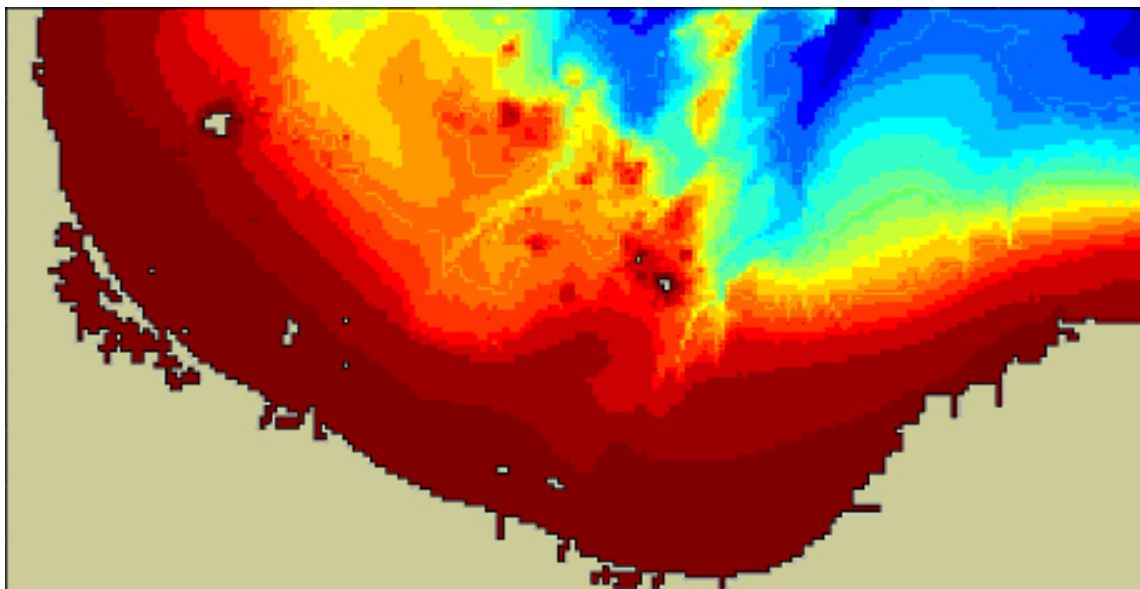


Numerical hydrodynamic modelling: Aquaculture Management Areas



For



Environment Bay of Plenty



October 2006

Numerical hydrodynamic modelling: Aquaculture Management Areas

Report Status

Version	Date	Status	Approved By:
V.1	September 2006	Draft	KPB
V.2	October 2006	Final	KPB

It is the responsibility of the reader to verify the currency of the version number of this report. All subsequent releases will be made directly to the Client.

The information, including the intellectual property, contained in this report is confidential and proprietary to ASR Limited. It may be used by the persons to whom it is provided for the stated purpose for which it is provided, and must not be imparted to any third person without the prior written approval of ASR. ASR Limited reserves all legal rights and remedies in relation to any infringement of its rights in respect of its confidential information.

© ASR Limited 2006

Acknowledgements

This work was conducted for Environment Bay of Plenty. EBOP staff participated in the collection of data. We particularly thank the EBOP Project Leader Stephen Park for his very helpful involvement and Shane Iremonger for his assistance with provision of data and field work. Others closely involved were Paul Dell and Aileen Lawrie. The co-operation of the University of Waikato Coastal Marine Group is also warmly acknowledged.

Numerical hydrodynamic modelling: Aquaculture Management Areas

Peter Longdill^{1,2}
Kerry Black¹

¹ ASR LTD, Marine Consulting and Research, 1 Wainui Rd, Raglan, New Zealand +64 7 8250380.

² Coastal Marine Group, University of Waikato, Private Bag 3105, Hamilton, New Zealand.

Report prepared for Bay of Plenty Regional Council

Executive Summary

Numerical hydrodynamic modelling of the Bay of Plenty was undertaken to be informed about offshore oceanographic and ecological systems for selection of open coast Aquaculture Management Areas which will sustain the environment, kaimoana and the aquaculture industry in the Bay of Plenty. The broad study involved:

- Establishing monitoring stations and undertaking regular surveys of water properties, currents and waves
- Undertaking numerical modelling of circulation and physical dynamics
- Undertaking numerical modelling of the food chain (food dynamics modelling), with particular focus on green mussels
- Developing recommendations about the carrying capacity of sites around the Bay of Plenty

The present report deals with the numerical modelling of hydrodynamics for the subsequent primary production modelling and the impacts of large scale green-lipped mussel farming within the Bay of Plenty. The goal of the current stage of the project was to calibrate the hydrodynamic model 3DD from the “3DD Suite”, which were:

- 2D – 2-dimensional circulation predicting the depth averaged currents.
- 3DHomo (barotropic) – 3-dimensional circulation models predicting the currents in several levels through the water column.
- 3DStrat (baroclinic) – 3-dimensional circulation models predicting the currents under salinity and temperature stratified conditions.

The third model is highly complex as the inputs to the model are multiple and time-varying over a large spatial scale. Challenges included establishment of initial conditions at the start of the model run (throughout the grid in each layer) and the determination of boundary conditions that specify sea levels, temperatures and salinities in the open boundary cells of the model.

After consideration and testing of several options, satellite observations were highly utilised, including the development of a novel temperature “nudging scheme”. This involved assimilation of satellite-sensed sea surface temperatures in the upper two layers of

the model, and applied every 3 days. By using the measured satellite temperatures, the model incorporates the elevated temperatures associated with the warm East Auckland current that penetrates into Bay of Plenty and the highly variable temperatures associated with shallow water heating/cooling and the upwelling that is common around East Cape. The satellite images reveal the complexity of the temperature structure in the Bay which is captured by assimilating the satellite data directly into the model. This novel method was developed for the study and has not been used in New Zealand modelling previously. In addition, satellite observations were used for determination of boundary conditions and river temperatures. Finally, the wind fields were also taken from satellite measurements at 14 sites across the model domain.

For the sea levels on the open boundaries, a “Coriolis Boundary” condition (uniquely provided by model 3DD) was adopted to enable accurate reproduction of the cross-shore geostrophically-balanced sea gradients that occur under winds on the continental shelf.

The final calibration results are shown in Figures 6.10-6.13. We found that the model was effectively reproducing the dynamics of the Bay of Plenty, including both the longshore and cross-shore currents throughout the water column. The salinities and temperatures were closely matching the field measurements.

Given the complexity of the environment, the good results are attributed to the quality of the field measurements, the intensity of the calibration and the capacity of the model to treat a broad range of processes simultaneously. The novel and extensive use of satellite observations also assisted greatly.

We conclude that the model is able to reproduce the essential dynamics of Bay of Plenty and can be applied to the determination of the potential environmental effects of the Aquaculture farms. In the next stage, the hydrodynamic model is used to drive the Primary Production model 3DDLlife, which considers impacts of the farms on the nutrients, phytoplankton and zooplankton in the Bay of Plenty due to mussel feeding.

Future hydrodynamic modelling would involve further comparisons with the very broad field dataset, including modelling over longer time periods, with detailed consideration of

continental shelf waves and the East Auckland current. Incorporation of these two phenomena would be expected to lead to further improvements in the model calibration.

Table of Contents

Executive Summary	iii
1 Introduction	1
1.1 Background – The Project	1
1.1.1 Studies undertaken.....	4
1.2 Background – Use of Field data for model calibration	5
1.3 Background – Report Structure	7
2 Numerical Modelling of the Bay Of Plenty.....	11
2.1 Numerical Model Description	11
3 Model domain and boundary conditions	17
3.1 Depth-averaged tidal modelling.....	18
3.2 Tidal model validation and residual current determination	19
3.2.1 Numerical Parameters	21
3.3 Determination of tidal and residual currents.....	23
4 Wind-driven circulation.....	25
4.1 Boundary Conditions	25
4.1.1 Wind Measurements	26
4.2 Calibration / Validation Data	29
4.3 Model Runs.....	29
4.4 Summary of 2D Calibration Runs.....	32
4.5 Westerly Currents	33
5 3D Homogenous Model Runs	36
6 3D Baroclinic Model Runs	40
6.1 Specifying Temperature and Salinity across the grid	40
7 Conclusions	60
8 References	61

List of Figures

Figure 1.1 - Proposed offshore aquaculture sites in the Bay of Plenty.....	3
Figure 1.2 - Locality map showing the nautical chart of the Bay of Plenty region (NZ54) with the model domain of 3DD modelling shaded red.....	5
Figure 3.1 - Model domain used to validate the numerical model. The model domain has open boundaries on the North and East boundaries.....	18
Figure 3.2 - The main oceanic currents around New Zealand (Source, http://www.starfish.govt.nz/shared-graphics-for-download/currents.jpg).....	19
Figure 3.3 - Deployment locations of ADP offshore from Pukehina and Opotiki. Also shown is the location of Moturiki Island, where the water level recorder is located.	20
Figure 3.4 - Correlation between measured and predicted water levels at Moturiki Island.....	21
Figure 3.5 – Tidally-generated currents within the Bay of Plenty at mid ebb stage.....	22
Figure 3.6 - Tidally generated currents within the Bay of Plenty at mid flood stage.	22
Figure 4.1 - Tauranga (left) and Whakatane (right) wind data from January 2003 to December 2004. Data from anemometers located at Tauranga and Whakatane Airports.....	27
Figure 4.2 – Tauranga airport measured wind velocities, inferred and interpolated QuikScat wind velocities (for a single point closest to Tauranga Airport), and the difference between them.....	28
Figure 4.3 - Run 002 results at the Pukehina ADP site. The model was driven with the Tauranga and Whakatane Winds scaled by a factor of 1.5. The offshore and alongshore components are relative to the bathymetry contours and coastline surrounding the ADP site.....	30
Figure 4.4 – QuikScat wind raw data (red points), 3 hourly spliner interpolated data (blue line) and the Tauranga airport wind records, directions relative to the Pukehina bathymetry and coastline.....	31
Figure 4.5 – Modelled currents from Run 7 – 14 QuikScat wind stations - and observed water currents from the ADP. Directions relative to the Pukehina bathymetry and coastline.....	31
Figure 4.6 – Run008, 14 QuikScat wind stations scaled to 0.8 of their original magnitude.....	32
Figure 4.7 – Velocity profiles from ADP current meter during times of depth averaged northwesterly flow. Velocities relative to coastline and bathymetry contours at Pukehina ADP site.	34
Figure 4.8 – Water temperatures at the Pukehina ADP site for the calibration period. Temperatures measured by TidBit® Stowaway temperature sensors. Missing data is due to servicing of the temperature string.....	35
Figure 5.1- Alongshore component of measured and modelled velocities Model is the smoother blue line. ...	38
Figure 5.2 - Offshore component of measured and modelled current velocities. Model is the smoother blue line.....	39
Figure 6.1 - Locations of measurements in September 2003.....	42
Figure 6.2- Combined OSD,CTD,XBT,PFL measurements from http://www.nodc.noaa.gov/cgi-bin/OC5/SELECT/dbextract.pl	43
Figure 6.3 – Typical profiles of temperature within the Bay of Plenty during the year. Green lines are summer time measurements, blue lines are spring and autumn measurements and red lines are winter measurements.....	44
Figure 6.4 – Assessed thermocline depth in the Bay of Plenty from numerous CTD casts over time.	44
Figure 6.5 - Temperatures recorded by satellite over a period of rapid warming. The plots show temperatures at 3 day intervals starting from October 18, 2004. Other features are the large variations that occur in shallow water near the coast and the upwelling along and around the tip of East Cape.....	45
Figure 6.6 - Alongshore model results from Run007.....	48
Figure 6.7 – On/offshore current velocities from Run007.....	49

Figure 6.8 - Temperatures from Run007. The red plotted points are the measured temperatures from the data collection programme, which show good correlation with the satellite observations (black line). The model (blue line) drifts and cools without assimilating the satellite data in the model.	50
Figure 6.9 - Salinities from Run007 with the recorded data at the Pukehina 50 m deep site. Salinity in the model is too low in the surface layers.	51
Figure 6.10 – Measured (black line) and modelled (blue line) offshore component of velocity at the Pukehina 50m site. The measured data has been filtered with a running mean filter with at window of 12 hours to reduce short term oscillations in the on-offshore flow. These short term oscillations are thought to be due to wave action or some other forcing which is not incorporated into the present model.....	55
Figure 6.11 – Measured (black line) and modelled (blue line) alongshore component of velocity at the Pukehina 50 m site in the Bay of Plenty.....	56
Figure 6.12 – Measured (black line) and modelled temperatures at the Pukehina 65m site. AVHRR Sea Surface Temperatures are also indicated at the surface layer with red dots.	57
Figure 6.13 – Measured (black dots) and modelled (blue line) salinities at the Pukehina 50m site. Salinities were measured with a Seabird CTD. Note that the constant nature of the modelled salinities for the first ~10 days is due to the ‘cold’ model start and the lag time for the reduced salinity water to reach this site.	58
Figure 6.14 – Measured (black squares) and modelled (main grid) surface salinities on 17 October 2003. Note that the general pattern of salinities is reproduced well by the model, with the exception of one ‘spurious’ data point off Opotiki.	59

List of Tables

Table 3.1 Descriptive information for the 3 km grid.....	21
Table 5.1 The 10 layers used in the 3DHomo simulations.....	36
Table 5.2 The 10 layers used in the 3DStrat simulations, with different layer interface positions to allow better representation of the temperature structure.	36
Table 6.1 Data collection sites. The columns 3k_i and 3k_j give the I and J coordinates of the sites in the 3 km grid.	40
Table 6.2 Best fit values of K_L (K_L) and K_S (K_S) for the measured profiles, obtained using the 1-d model. The measurement sites are identified as OPO: Opotiki, PUK: Pukehina, WHK: Whakatane and the depth at the site.	53

1 Introduction

1.1 BACKGROUND – THE PROJECT

New Zealand has been experiencing a rapid growth in the aquaculture industry in recent years. This growth, coupled with outdated legislation has prompted the government to reform the aquaculture legislation. The reforms took effect on 1 January 2005, amending five different Acts:

- Resource Management Amendment Act (No 2) 2004
- Fisheries Amendment Act (No 3) 2004
- Conservation Amendment Act 2004
- Biosecurity Amendment Act 2004
- Te Ture Whenua Maori Amendment Act (No 3) 2004

It also created two new Acts:

- Maori Commercial Aquaculture Claims Settlement Act 2004
- Aquaculture Reform (Repeals and Transitional Provisions) Act 2004

Under the new laws, new marine farms can now only be established within zones called Aquaculture Management Areas (AMAs). An AMA must be a defined area, mapped and described in the regional coastal plan. In considering AMAs, councils must consider the effects of aquaculture on the environment, fisheries resources, fishing interests and other uses of the coastal marine area. One of the central considerations in establishing AMA's is sustainability of the natural resources. This creates a need for a scientifically defensible understanding of the physical interactions in the offshore environment and the likely effects of any proposal.

Recent advances in technology coupled with pressure for space within the coast has seen proposals for large offshore farms. A single mussel farm of 4,750 ha has interim approval (Mfish Interim decision 2006) offshore from Opotiki (Figure 1.1). A further pre-moratorium mussel farm application for 3,800 ha near Pukehina/Otamarakau, in the central Bay of Plenty is yet to be heard (Figure 1.1). While there are many uncertainties with the expansion of aquaculture in the Bay of Plenty, there are many opportunities for

both filter feeders and other species. As the Regional Council are in the “driving” seat for planning for aquaculture, a robust and defensible understanding of the offshore Bay of Plenty is needed. This work provides a basis for decisions for the understanding of how marine farming is likely to affect the physical dynamics and biological values of the Bay of Plenty.

If aquaculture is to be advanced in the Bay of Plenty the council needs to:

- Ensure the current proposals are monitored and are sustainable; and
- Make decisions about other sites suitable for aquaculture, which sustain the environment and lead to an effective aquaculture industry.

Mussels and other filter feeders are known to extract both phytoplankton and zooplankton from the water column. Moreover, most nutrients arriving at the coast come from deeper water in the bottom mixed layer (Park, 1998) (Fig. 1.1). To reach the coast, this nutrient-rich seawater must pass through the AMAs and so impacts on the inshore wider environment need to be understood.

The goals of this project were to provide focused information over-viewing the Bay of Plenty for planning of AMAs. The aims were achieved by establishing data collection programmes coupled with sophisticated numerical models. Thus, any scenario can be modelled to provide information on the likely effects.

Regional councils are also obliged to monitor cumulative effects of activities. This work also can be readily absorbed into the regional monitoring programs or for particular farms.

This information provides significant potential benefits to the aquaculture industry by providing background information on the nature of the offshore environment and providing the tools by which effects of any proposal can be assessed.

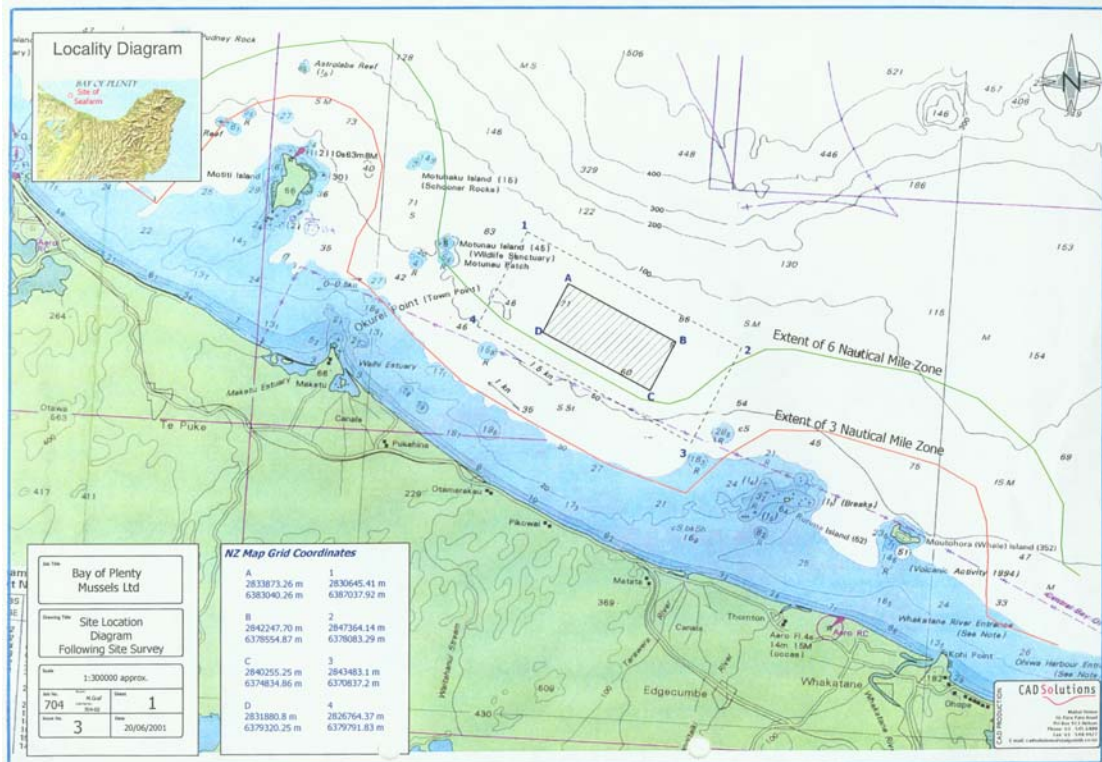
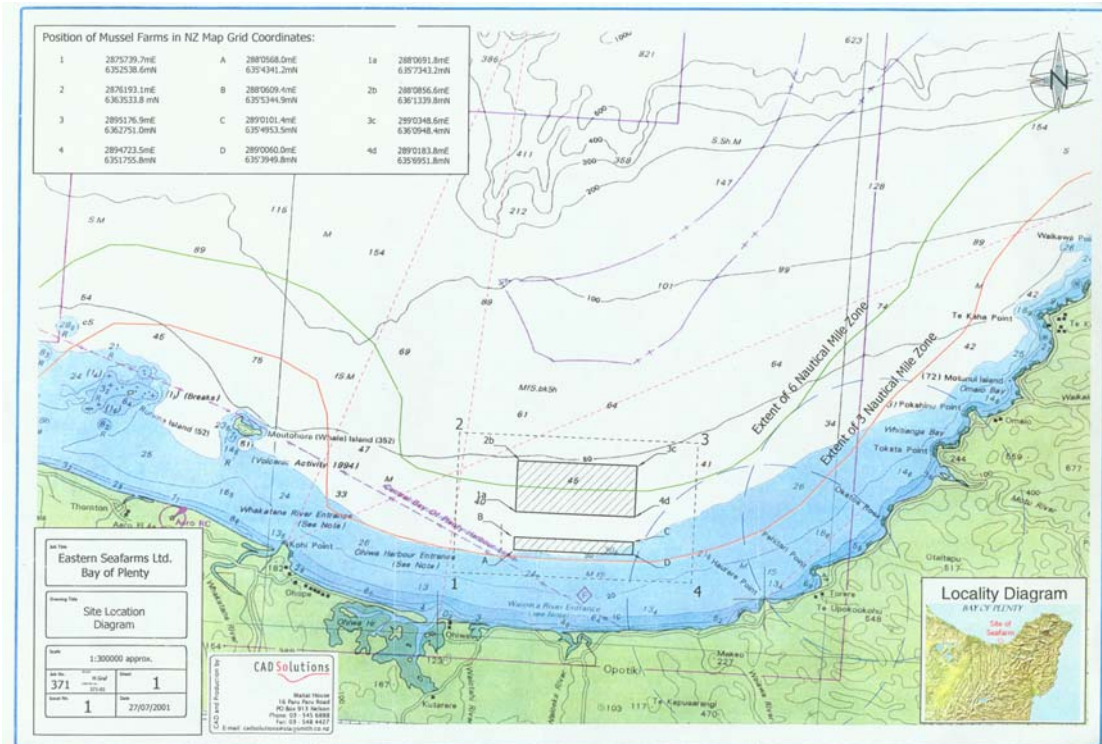


Figure 1.1 - Proposed offshore aquaculture sites in the Bay of Plenty

1.1.1 Studies undertaken

To redress the lack for data and understanding of the system, EBoP commissioned ASR Ltd as follows:

- To be informed about offshore oceanographic and ecological systems when choosing open coast AMA sites, for a sustainable environment, kaimoana and aquaculture industry in the Bay of Plenty

The goals were achieved by:

- Establishing monitoring stations and undertaking regular surveys of water properties, currents and waves
- Undertaking numerical modelling of circulation and physical dynamics
- Undertaking numerical modelling of the food chain (food dynamics modelling), with particular focus on green mussels
- Developing recommendations about the carrying capacity of sites around the Bay of Plenty

The present report deals with the numerical modelling of hydrodynamics for the subsequent primary production modelling and the impacts of large scale green-lipped mussel farming within the Bay of Plenty (Figure 1.2). While AMA designation within the Bay of Plenty system could be used for a variety of different aquaculture types e.g., sponge, scallop, fin-fish and mussel aquaculture, this study has used mussel aquaculture to examine likely effects on primary production and carrying capacity. This is predominantly due to large mussel farms representing the present applications, and the fact that mussel culture has received the most attention with respect to effects on primary production and carrying capacity and as such, useful benchmarks using chlorophyll *a* levels have been derived for determining likely impacts and effects (e.g., Inglis *et al.* 2005). Mussels feed on phytoplankton, zooplankton, detritus and other organic particles in the

size-range 3-200 μm . which they filter from the water column, and large mussels can filter up to 350 liters of water per day.

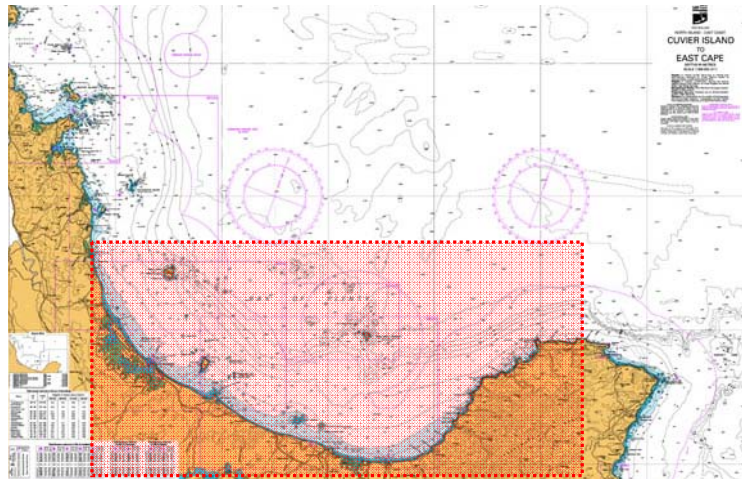


Figure 1.2 - Locality map showing the nautical chart of the Bay of Plenty region (NZ54) with the model domain of 3DD modelling shaded red.

1.2 Background – Use of Field data for model calibration

A large amount of field data was recorded for this study over 2 years. The list of reports that are relevant to the study are listed below:

- Black, K.P., Beamsley, B., Longdill, P., Moores, A., 2005 *Current and Temperature Measurements: Aquaculture Management Area*. Report prepared by ASR Consultants for Bay of Plenty Regional Council, March 2005.
- Longdill, P.C., Black, K.P., Park, S. and Healy, T.R., 2005. *Bay of Plenty Shelf Physical and Chemical Properties 2003-2004 : Choosing open coast AMAs to sustain the environment, kaimoana and aquaculture industry*. Report for Environment Bay of Plenty, ASR Ltd, P.O. Box 67, Raglan, NZ, and the University of Waikato. 35p

- Longdill, P. C., and Black, K. P., and Healy, T.R. 2005. *Locating aquaculture management areas – an integrated approach*. Report for Environment Bay of Plenty, ASR Ltd, P.O. Box 67, Raglan, NZ, and the University of Waikato. 53p.
- Longdill, P.C., Black, K.P., Haggitt, T. and Mead, S.T., 2006. *Primary Production Modelling, and Assessment of Large Scale Impacts of Aquaculture Management Areas on the Productivity within the Bay of Plenty*. Report for Environment Bay of Plenty, ASR Ltd, PO Box 67, Raglan, New Zealand. 51p
- Mead, S.T., Longdill, P.C., Moores, A., Beamsley, B., and Black, K.P. *Underwater Video, Grab Samples and Dredge Tows of the Bay of Plenty Sub-Tidal Area (10-100 m depth)*. Report for Environment Bay of Plenty, ASR Ltd, PO Box 67, Raglan, New Zealand. 34p
- Park, S.G. and Longdill, P.C. 2006. Synopsis of SST and Chl-a in Bay of Plenty waters by remote sensing. *Environment BOP Environmental Publication 2006/13. Environment Bay of Plenty, PO Box 364, Whakatane.*
- Black, K.P., Haggitt, T., Mead, S.T., Longdill, P., Prasetya, G. and Bosserelle, C., 2006. *Bay of Plenty Primary Production Modelling: Influence of climatic variation and change*. Report for Environment Bay of Plenty, ASR Ltd, PO Box 67, Raglan, New Zealand. 43p.
- Richardson, K.M, Pinkerton, M.H., Uddstrom, M.J., Gall, M.P., Hill, P. 2005. *Remote sensing survey of the Bay of Plenty: Report on sea surface temperature and ocean colour product generation for Environment Bay of Plenty*. NIWA Project EBP04302.

The data coming from these studies was used for the calibration of the numerical models, by comparing model results with field measurements. In this report, only a subset of the data and calibration is presented. However, many other comparisons were made and these provided further confidence in the model calibration. The study also forms the basis for a

PhD degree investigation of Mr Peter Longdill who is being jointly supervised by Prof Terry Healy at University of Waikato and Dr Kerry Black at ASR Ltd. Additional comparisons with the model will form a segment of the PhD which is anticipated to be completed towards the end of 2007.

1.3 Background – Report Structure

This report presents the numerical hydrodynamic modelling undertaken for the Aquaculture Management Area Study. The goal is to specify circulation for application to the primary production modelling which will be used to investigate the effect of the farms on the broader environment. Currents determine the rate of delivery of new nutrients to aquaculture sites and act to flush the farmed zones. In addition, the currents transmit the effects of farms to other regions. For example, water bodies with substantially reduced nutrients or phytoplankton transmitted by currents into the coastal zone, marine parks etc. could allow the farms to have an impact broader than their immediate environs.

In the field data report (Longdill et al., 2005), the inner shelf is shown to be highly dynamic and variable, both in space and time. Such a system can be treated using high quality numerical models that simultaneously deal with the multiple processes driving the circulation.

Numerical hydrodynamic models (HD models) fall into several categories of increasing complexity. These are

- 2D – 2-dimensional circulation models predicting the depth averaged currents. These show the general horizontal circulation patterns but they cannot effectively predict the important processes of up/downwelling which bring nutrient rich bottom waters from the deep ocean to the coast.
- 3DHomo – 3-dimensional circulation models predicting the currents in several levels through the water column. While these are an improvement over the 2D model in their predictive capability, they do not treat the stratification of the water

column, associated with either fresh water surface layers due to river inputs or thermoclines that form under solar radiation inputs to the water column

- 3DStrat – 3-dimensional circulation models predicting the currents in stratified conditions. These models are highly complex as the inputs to the model are multiple and time-varying. The model predicts the stratification by including the effects of buoyancy and density. Key inputs are (1) the river flows that determine the inputs of freshwater and the formation of plumes and (2) the solar radiation that forms the temperature stratification identified in the field measurements. The latter is known as an ocean/atmosphere model which predicts the exchanges of heat between the atmosphere and the ocean. Such models have been rarely applied to NZ water bodies (e.g. Black et al., 1996) and so the modelling is leading edge and challenging.

To calibrate a model, it is necessary to work through an iterative process of adjustment of the coefficients in the model (such as mixing / friction) until a best fit with the measured data is achieved. The model is then validated by keeping the coefficients the same and simulating a different period in time.

While this process of calibration/validation is standard in modelling, it is actually not the most substantial part of the work in complex models such as 3DStrat. For 3DStrat, the modeller must have a good knowledge of the system to produce the detailed information needed to run the model as actual measurements are not available across the full domain of the model grid. The following information is needed for 3DStrat.

Water level, temperature and salinity boundary conditions around the entire open perimeter of the model grid. This requires the modeller to prescribe the boundary conditions at each model cell every time step (about every 10 s), which is a very large amount of information at a fine spatial scale. To measure such data is not possible (cost prohibitive, particularly in over 1000 m of water) and so the challenge of the modeller is to find best ways to form the boundary conditions using a blend of measurements and

oceanographic general knowledge. Such work requires a high level of understanding of physical oceanography and the ability to deal effectively with diverse datasets.

Initial conditions for temperature and salinity at all model cells. When the model starts at a selected time zero, initial conditions for all variables are required throughout the grid in every model cell (some 25,530 cells). Of course, measurements are not available and so the challenge of the modeller is to form the most effective initial condition from the available information. The most difficult variables are the temperature and salinity as any initial offset in these values will be carried through the full model run and lead to offsets from the measurements. Also, incorrect initial conditions will cause the model to misrepresent the dynamics or even “crash”, i.e. go fully out of range and create erroneous solutions. Notably, while not the subject of this report, the same issues of suitable initial conditions arise in the primary production modelling.

Ocean/atmosphere variables. To treat the thermal ocean/atmosphere coupling, the model requires time series across the grid of winds, solar radiation, barometric pressure, relative humidity, cloud cover and air temperature. Of course, such measurements are not available at all locations in the grid and indeed many are measured only on land, while the model will operate most effectively if the measurements are provided over water. One of the challenges of the study was to most effectively determine the required values using a breadth of datasets and then to test the effectiveness by running the model and comparing outputs to measurements. Ultimately, the logical choices gave the best results (this included using satellite measured winds and sea surface temperatures over the grid) but some improvement to the model may still be achieved with more detailed input information.

Several novel approaches not used previously in New Zealand were adopted. Amongst these was the incorporation of a satellite sea surface temperature “nudging” scheme. The ocean temperature changes are determined in practice by the small difference between a series very large terms in the ocean/atmosphere equations. Any deviation in the large terms will lead to an imbalance that is identified in the model by a drift in the

temperatures over long model runs, i.e. nett heat loss or gain over the model simulation until eventually the whole model grid is too hot or too cool. Given the uncertainty in the inputs, such trends cannot be cured solely by simply adjusting the model coefficients, as the multiple terms in the heat equations interact with each other in a complex fashion. For example, wind induces substantial heat losses and so the wind measurements are critical to the success of the modelling. However, adjustments to the wind for heat losses to allow for drifts over the grid, may also lead to incorrect predictions of the wind driven currents. To overcome this difficulty, we developed the nudging scheme, whereby the sea surface temperatures recorded every 3 days (approx) by satellite were applied to the top layers of the model to keep the temperature on track. This method allows the modelling to occur over long time periods (e.g. a full year) without a drift in the temperatures and was found to be highly practical and will be generally applicable to other regions around New Zealand in the future.

In this report, we work through the various levels of complexity of the models from 2D to 3DStrat. We chose to examine each in turn as the process provided a means to determine the accuracy of each type of model, while unravelling the underlying causes of deviations between the model and measurements. The systematic approach gives better insights into the dynamics and helps the modeller and reader to become aware of the forces driving the dynamics of the Bay of Plenty.

Data for calibration was available on transects and from long-term moorings as described by Longdill et al. (2005) and Beamsley et al. (2005).

The structure of the report is as follows;

- Section 1** Introduction and background to the project
- Section 2** Numerical model description
- Section 3** Tidal model validation and calibration
- Section 4** Wind Driven circulation
- Section 5** 2D modelling
- Section 6** 3D modelling

2 Numerical Modelling of the Bay Of Plenty

2.1 Numerical Model Description

The numerical model adopted in the study is 3DD (© Black 2001) which has been applied and calibrated for New Zealand and international water bodies on numerous occasions since the early 80's. The 3DD Suite is a commercial package of models sold worldwide and deals with all physical processes from sediment transport to oil spills, beach dynamics, waves and currents. In this report we adopt the flagship hydrodynamic model 3DD, which incorporates capacity from 2D to 3DStrat. The model 3DD is based on the momentum and conservation of mass (continuity) equations, as most recently described by Black et al. (2005).

An explicit finite difference (Eulerian) solution is used to solve the momentum and continuity equations for velocity and sealevel, through a series of vertical layers that are hydrodynamically linked by the vertical eddy viscosity. The model provides for spatial variation in roughness length (z_0) and horizontal eddy viscosity (A_H). Non-linear terms and Coriolis force can be included or neglected, while the land/sea boundaries can be set to free slip or no-slip.

The model 3DD has been successfully applied and verified in a diverse range of situations (Black 1987; Black 1989; Black and Gay 1991; Black et al. 1993; Young et al. 1994; Middleton and Black 1994). The model has been previously applied to investigate the parameters responsible for eddy formation behind islands and reefs (Black and Gay 1987; Black 1989; Hume et al. 2000). The equations of horizontal motion for an incompressible fluid on a rotating earth in Cartesian coordinates with the z axes positive upward are:

$$\frac{\partial u}{\partial t} + u \frac{\partial u}{\partial x} + v \frac{\partial u}{\partial y} + w \frac{\partial u}{\partial z} - fv = -g \frac{\partial \zeta}{\partial x} - \frac{1}{\rho} \frac{\partial P}{\partial x} + A_H \left(\frac{\partial^2 u}{\partial x^2} + \frac{\partial^2 u}{\partial y^2} \right) + \frac{\partial}{\partial z} \left(N_z \frac{\partial u}{\partial z} \right) \quad (1)$$

$$\frac{\partial v}{\partial t} + u \frac{\partial v}{\partial x} + v \frac{\partial v}{\partial y} + w \frac{\partial v}{\partial z} + fu = -g \frac{\partial \zeta}{\partial y} - \frac{1}{\rho} \frac{\partial P}{\partial y} + A_H \left(\frac{\partial^2 v}{\partial x^2} + \frac{\partial^2 v}{\partial y^2} \right) + \frac{\partial}{\partial z} \left(N_z \frac{\partial v}{\partial z} \right) \quad (2)$$

$$w = -\frac{\partial}{\partial x} \int_{-h}^z u dz - \frac{\partial}{\partial y} \int_{-h}^z v dz \quad (3)$$

t is the time, u , v are horizontal velocities in the x , y directions respectively, w the vertical velocity (positive upward), h the depth, g the gravitational acceleration, ζ the sea level above a horizontal datum, f the Coriolis parameter, P the pressure, A_H the horizontal eddy viscosity coefficient, and N_z the vertical eddy viscosity coefficient and ρ is the density which varies with depth.

Assuming that vertical acceleration is neglected, the hydrostatic equation for the pressure at depth z is:

$$P = P_{atm} + g \int_z^{\zeta} \rho dz \quad (4)$$

where P_{atm} is the atmospheric pressure.

The physical representations of each of the various terms in the momentum equation are: local acceleration; inertia; Coriolis; pressure gradient due to sea level variation; pressure gradient due to atmospheric pressure; wind stress and bed friction; horizontal eddy viscosity. A_H varies spatially but the gradients are assumed to be small. Atmospheric pressure changes were not included in the simulations and therefore this term in the momentum equation is neglected.

The salt and heat balance component of the model is coupled to the hydrodynamics through the application of the baroclinic pressure gradient associated with the horizontal temperature and/or salinity density field. The advection/diffusion equations are solved on

the same grid as the hydrodynamics using a second-order-accurate, explicit, finite difference solution. The conservation equations for temperature and salinity may be written as:

$$\frac{\partial T}{\partial t} + u \frac{\partial T}{\partial x} + v \frac{\partial T}{\partial y} + w \frac{\partial T}{\partial z} = \frac{\partial}{\partial z} \left(K_z \frac{\partial T}{\partial z} \right) + K_H \left(\frac{\partial^2 T}{\partial x^2} + \frac{\partial^2 T}{\partial y^2} \right) \quad (5)$$

$$\frac{\partial S}{\partial t} + u \frac{\partial S}{\partial x} + v \frac{\partial S}{\partial y} + w \frac{\partial S}{\partial z} = \frac{\partial}{\partial z} \left(K_z \frac{\partial S}{\partial z} \right) + K_H \left(\frac{\partial^2 S}{\partial x^2} + \frac{\partial^2 S}{\partial y^2} \right) \quad (6)$$

where T is temperature, S is salinity, and K_H , K_z are the horizontal and vertical coefficients of eddy diffusivity.

The density is computed according to an equation of state of the form,

$$\rho = \rho(T, S, z) \quad (7)$$

The boundary conditions at the free surface $z = \eta$ are:

$$N_z \frac{\partial u}{\partial z} = \tau_x^s \quad N_z \frac{\partial v}{\partial z} = \tau_y^s \quad \frac{\partial \zeta}{\partial t} + u \frac{\partial \zeta}{\partial x} + v \frac{\partial \zeta}{\partial y} = w^s \quad (8)$$

where τ_x^s, τ_y^s denotes the components of wind stress, w^s is the vertical velocity at the surface, and

$$\tau_x^s = \rho_a \gamma |W| \frac{W_x}{\rho} \quad \tau_y^s = \rho_a \gamma |W| \frac{W_y}{\rho} \quad (9)$$

ρ is the water density, W the wind speed at 10 m above sea level while W_x and W_y are the x and y components, γ is the wind drag coefficient, ρ_a the density of air.

The wind drag coefficient comes from the work of Wu (1982) where the drag coefficient

γ is of the form,

$$\square = (0.8 + 0.065 W_s) \times 10^{-3} \quad (10)$$

where W_s is the numerical value in m.s^{-1} of the wind speed at 10m above sea-level.

Surface boundary conditions for salinity S_l and temperature T_l are,

$$N_z \frac{\partial S}{\partial z} = S_l \quad N_z \frac{\partial T}{\partial z} = T_l \quad (11)$$

where,

$$S_l = S_0 (E_l - P_l) / \square \text{ and } T_l = Q/c \quad (12)$$

and S_0 is the surface salinity, E_l is the net evaporation, P_l is the net precipitation mass flux of fresh water, Q is the net ocean heat flux and c is the water heat capacity.

Assuming seabed slope is small, at the sea bed, $z = -h$, we have

$$N_z \frac{\partial u}{\partial z} = \tau_x^h \quad N_z \frac{\partial v}{\partial z} = \tau_y^h \quad (13)$$

where τ_x^h, τ_y^h denotes the components of bottom stress. Applying a quadratic law at the sea bed,

$$\begin{aligned} \tau_x^h &= g u_h (u_h^2 + v_h^2)^{1/2} / C^2 \\ \tau_y^h &= g v_h (u_h^2 + v_h^2)^{1/2} / C^2 \end{aligned} \quad (14)$$

with u_h, v_h being the bottom currents and C is Chezy's C. For a logarithmic profile,

$$C = 18 \log_{10}(0.37 h/z_o) \quad (15)$$

where z_o is the roughness length.

The equation of state in a salinity-stratified condition can be approximated as,

$$\rho = \rho_0 + \rho S \quad (16)$$

where ρ is 0.74 at 20°C and ρ_0 is the density of freshwater (1000 kg.m⁻³).

The equation of state in a temperature and salinity stratified condition can be approximated as

$$\rho = 1000 (1.0 - 3.7 \times 10^{-6} T^2 + 8.13 \times 10^{-4} S) \quad (17)$$

where $T = T' + 2.7$ and T' is the temperature in °C, S is the salinity (typically 35).

For the temperature-stratified simulations, the vertical eddy viscosity and diffusivity is based on a mixing length and Richardson number formulation, as

$$l_m(z) = \kappa z \left(1 - \frac{z}{h}\right) \quad \text{and} \quad N_0(z) = l_m^2 \left[\left(\frac{\partial u}{\partial z}\right)^2 + \left(\frac{\partial v}{\partial z}\right)^2 \right]^{1/2} \quad (18)$$

where $N_0(z)$ is either the eddy viscosity N_z or eddy diffusivity K_z at elevation z above the sea bed, l_m is the mixing length, and κ is the Von Karman constant set to 0.4. In stratified flows, the gradient Richardson Number is,

$$R_i(z) = \left(g \left(\frac{\partial \rho}{\partial z} \right)^2 / \left(\frac{\partial u}{\partial z} \right)^2 \right) \quad (19)$$

To determine the reduced vertical eddy viscosity and diffusivity in stratified flows, we use the Perrels and Karelse (1982) formula,

$$N_{(z)} = N_{0(z)} e^{-\alpha R_i(z)} \quad (20a)$$

$$K_{(z)} = K_{0(z)} e^{-\alpha R_i(z)} \quad (20b)$$

where $\alpha = 4$ and 12 for the eddy viscosity and eddy diffusivity respectively.

To solve the equations by the finite difference method, a staggered finite difference grid is utilised similar to that applied by Leendertse and Liu (1975). The sea level replaces w in the top layer. The solution is found by time stepping with a 2nd order-accurate explicit scheme and third-order approximations for the non-linear inertia terms.

Z-coordinate is favoured over a sigma co-ordinate model to eliminate problems encountered when representing horizontal density gradients in a grid with non-horizontal grid cells. Similarly at the seabed, layered models typically represent a sloping seabed by a series of steps, with approximate heights equal to the model's vertical grid size. In baroclinic simulations, this can create local upwelling at the step walls, which is an artefact of the model's vertical resolution. These local upwellings can penetrate through the water column, causing a pattern of false internal wave activity. In 3DD, the depth is reproduced accurately by allowing fractionated cell sizes at the bed, which are less than the vertical grid size. The merits of the scheme have been assessed by simulating the steep profile used by Lamb (1994) to examine soliton formation. With the fractionated depth scheme, the velocities on the steeply-rising "continental shelf" varied smoothly in the model. Other aspects of the model of relevance to the Bay of Plenty region are described by Black et al. (2000) who consider the 3-dimensional baroclinic circulation of the nearby Hauraki Gulf.

3 Model domain and boundary conditions

The model computational domain was selected to cover the entire Bay of Plenty, extending from The Coromandel Peninsula in the west to East Cape in the east (Figure 1.2). The domain included all offshore islands and reef systems within the defined area. For initial model calibration purposes the grid resolution was 1000x1000 m. For later investigations into three-dimensional circulation within the Bay of Plenty, a coarser grid of 3000x3000 m was used. While the latter is coarse compared to estuarine models, it was found through sensitivity testing that the results were very similar between the 1 km and 3 km grids. This occurred because the bathymetric features to be represented by the model are large scale and can be adequately reproduced on a 3 km grid. Further refinement of the grid in future may be justified by high resolution field measurements.

The model grid used the EBOP depth database, which holds some 330,000 individual depth measurements over the Bay. The database was formed from a variety of sources and checked thoroughly for outliers by EBOP prior to release. Many interesting features can be seen in this exceptionally high-resolution dataset, including what look like drowned rivers on the outer edge of the shelf (e.g. Figure 3.1). To create the model grids, the XYZ files (of latitudes, longitudes and depths) were first converted into metric position coordinates (NZMG1949) and then gridded using the commercial package ©Surfer. In the last stage, the Surfer files are converted to model bathymetry files using the Support Tools in the 3DD Suite.

The model domain has two open boundaries for which boundary conditions are required; an Eastern and a Northern boundary (Figure 3.1). Notably, the most difficult numerical simulations are those on an open coast, due to the complexity of the circulation and the many factors that drive the currents including large-scale ocean forcing, ocean currents, thermal and freshwater stratification, wind, coastal-trapped waves, barometrically-induced and Coriolis-induced flows and tides. The East Auckland current also penetrates into the Bay from the north at times (Figure 3.2).

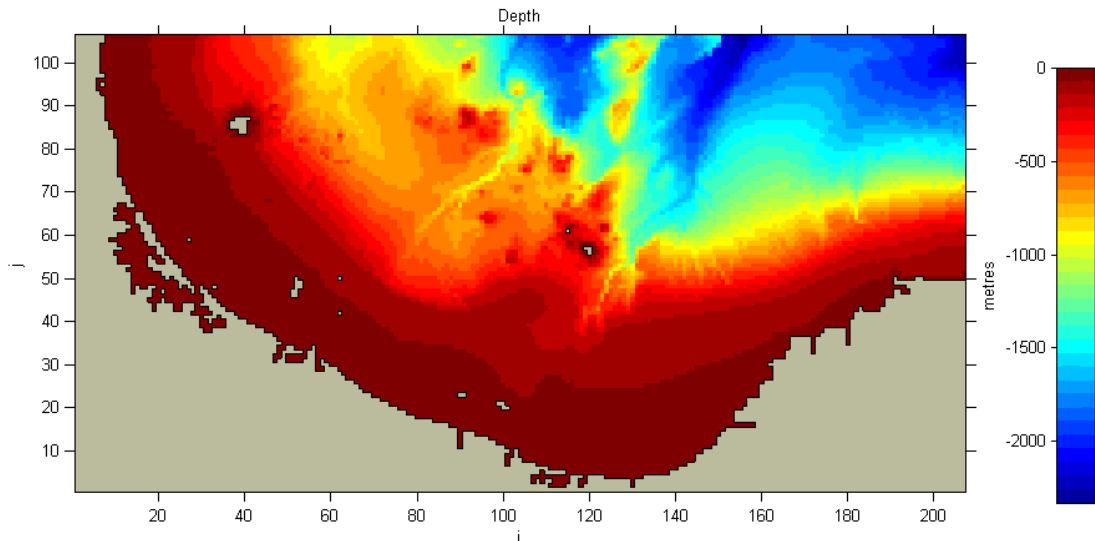


Figure 3.1 - Model domain used to validate the numerical model. The model domain has open boundaries on the North and East boundaries.

3.1 Depth-averaged tidal modelling

ASR's purpose-written software provides the ability to rapidly generate boundary conditions anywhere in the world for the 3DD suite of numerical models. The software utilises predictions of sea levels and velocities from a global tidal model (OSU Tidal Inversion Software (OTIS)). OTIS is a package of programs for tidal data assimilation based on methods used by Egbert et al., (1994), for the global inverse solution. OTIS applies a generalised inverse method, which allows the combination of all the available information into global tidal fields, best fitting both the data and the dynamics, in a least squares sense.

For the Bay of Plenty model on the 1000x1000 m model grid, water-level fluctuations were adopted along the northern boundary and momentum fluxes along the eastern boundary. Both boundary conditions were derived using all 10 of the available tidal constituents from the world tidal model.

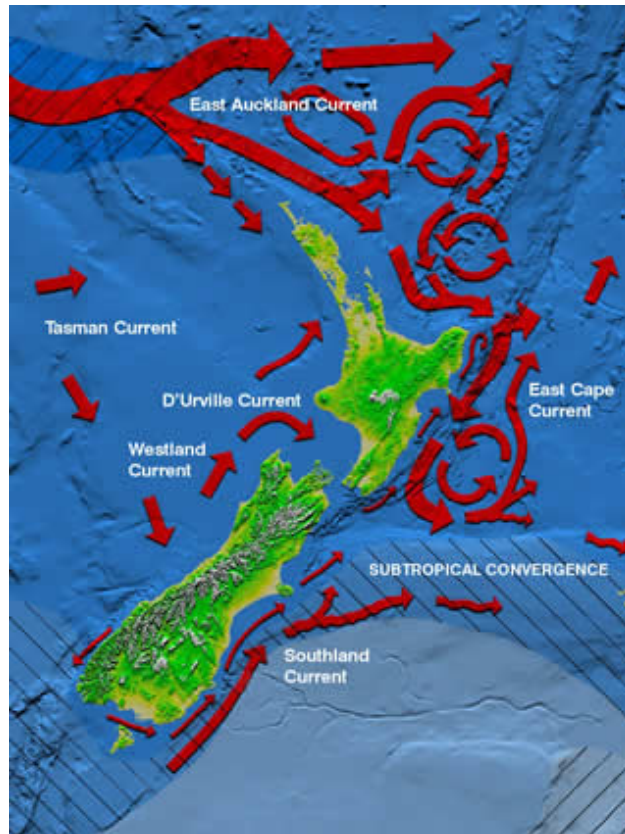


Figure 3.2 - The main oceanic currents around New Zealand (Source, <http://www.starfish.govt.nz/shared-graphics-for-download/currents.jpg>)

3.2 Tidal model validation and residual current determination

The time-series of the measured depth-averaged current velocities at both the Pukehina and Opotiki ADP sites (Figure 3.3) are too short to accurately resolve all the necessary tidal constituents required to separate the tidal and residual component of the measured data. Consequently, we calibrated water levels against the Moturiki tide gauge, which is a long-term monitoring site centred within the model grid and against the coast (Figure 3.3). The water levels recorded at Moturiki include both the oscillations in the water level due to tidal fluctuations, and the residual variations in the water level due to other processes, including atmospheric conditions, wind set-up etc (Figure 3.4). A tidal analysis provided separated time series of the tidal water levels and the “residual” water levels. These can then be used to validate the various numerical models described below.

Two parameters within the 2D numerical model must be adjusted during the calibration stage; the friction coefficient and eddy viscosity. Other parameters need to be calibrated in the more complex 3D models.

On completion of sensitivity testing, good correlation between the predicted and observed water levels is shown in Figure 3.4. As the tidal currents are very slow (Figure 3.5 and Figure 6), the results were not very sensitive to either the friction or the eddy viscosity magnitude. The dominant factor was the tidal boundary condition, and so the good results demonstrate the accuracy of the world tidal model and the adopted procedures of assimilation.

The value applied for the friction coefficient was $z_0=0.001$ m which is a standard magnitude for estuaries in 3DD. The horizontal eddy viscosity was $100 \text{ m}^2\text{s}^{-1}$. This is a relatively high value and so it is re-examined later in the 3DStrat modelling, where the river plumes are sensitive to the eddy viscosity and eddy diffusivity. Constant values for both parameters were applied universally over the grid in the absence of alternative field data and the lack of sensitivity of the model to the coefficients.



Figure 3.3 - Deployment locations of ADP offshore from Pukehina and Opotiki. Also shown is the location of Moturiki Island, where the water level recorder is located.

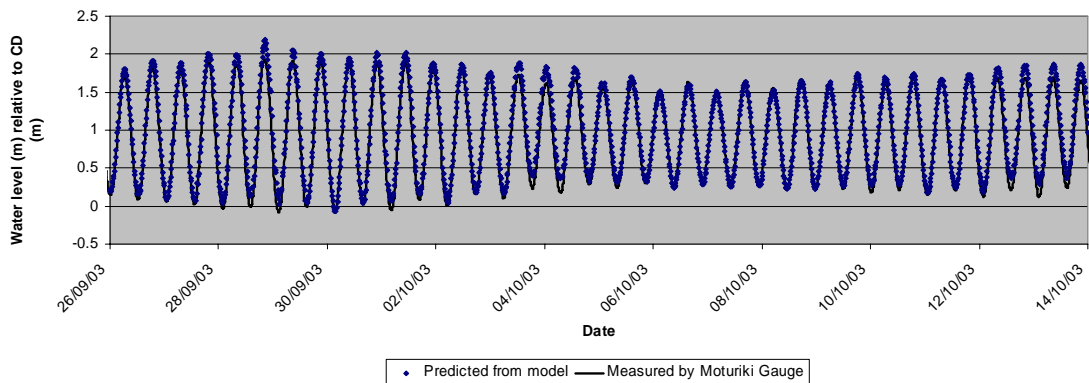


Figure 3.4 - Correlation between measured and predicted water levels at Moturiki Island

3.2.1 Numerical Parameters

Table 3.1 Descriptive information for the 3 km grid

Time step	10 seconds
Roughness length	0.001 m
Horizontal Eddy Viscosity	100 m ² s ⁻¹
Initial model start time	26 September, 2003 at 0 hours
Coast direction for Pukehina	118.7°
Coastal Slip	100%
Grid Latitude (centre)	-37°
Effective Depth	0.3 m
Drying Height	0.05 m
Grid cell sizes	3000 x 3000 m
Number of IJ cells	69,37
IJ at origin	1,1
Coordinate system	NZMG1949
X,Y at origin	2761000 mE, 6342000 mN
Grid orientation	0°

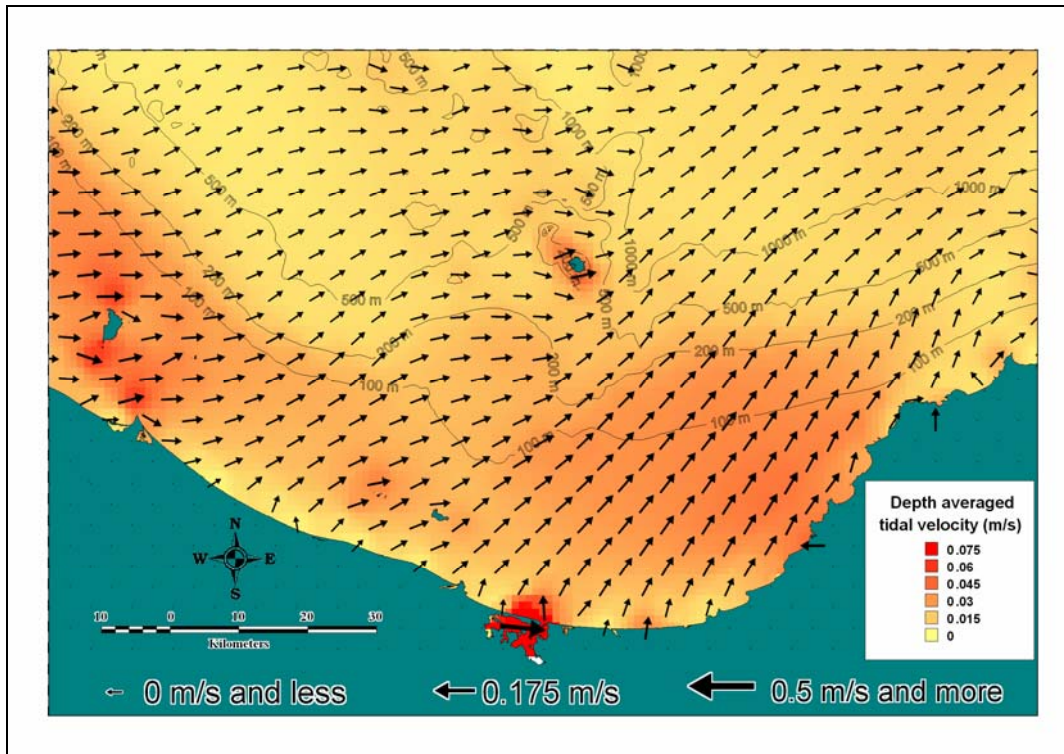


Figure 3.5 – Tidally-generated currents within the Bay of Plenty at mid ebb stage.

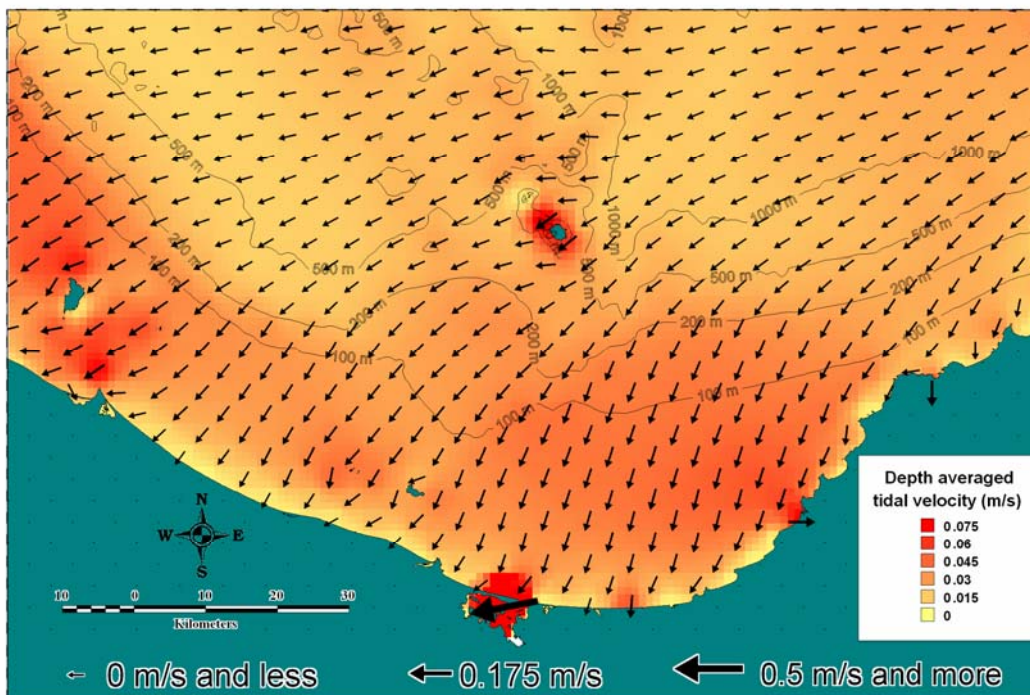


Figure 3.6 - Tidally generated currents within the Bay of Plenty at mid flood stage.

3.3 Determination of tidal and residual currents

With confidence in the results and boundary conditions, the numerical model 3DD was used to simulate tides for a period of ~3-months which was sufficient to allow the determination of sea level and current tidal constituents at both the Pukehina and Opotiki ADP deployment sites. The modelling allowed tides and residuals in the short records to be isolated, which could not be achieved without the support of the modelling.

Specifically, the determined tidal constituents are used to predict tidal velocities at the deployment sites and, by subtracting the tidally induced currents from the raw current data, the residual current velocities can be determined. The determined tidal constituents at both the Pukehina and Opotiki ADP sites are given in Appendix 1. The raw measured, tidal and residual current velocities (in both North and East components) for the first two deployments of the ADP at the Pukehina site are shown in Figure 6.

Notably, for the easterly component, the tidal current velocities are significantly smaller than the residual currents. Further, the easterly component (approximately longshore) of the velocity field is an order of magnitude larger than the north-directed velocity (approximately on/offshore) component (Figure 3.7).

As the residual currents are substantially faster than the tidal currents, the dominant mechanism for flushing and transmission of nutrients around the Bay is the residual circulation. As such, the study now focuses on these currents and their prediction.

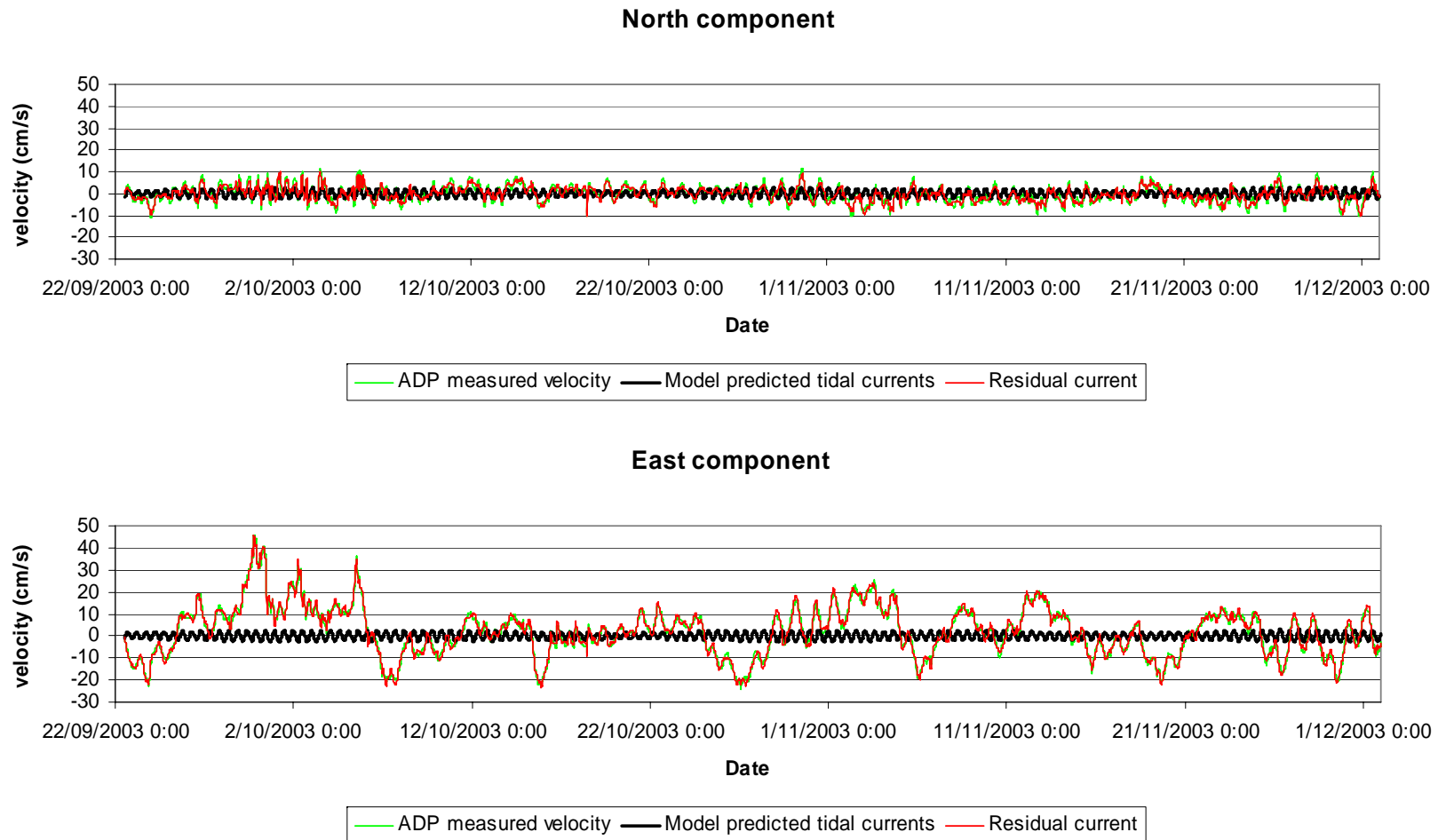


Figure 3.7 - Measured depth averaged current velocities (in North and East components) at Pukehina, validated model predicted tidal velocities and residual current velocities.

4 Wind-driven circulation

4.1 Boundary Conditions

For the wind-driven modelling, different methods need to be adopted for the open boundaries located at the north and east of the grid. Most importantly, geostrophy leads to substantial cross-shore gradients in the water levels when winds blow along the coast. Without an allowance for this in the boundary condition, the currents will be poorly predicted, particularly near the land. It is difficult, however, to forecast the sea level gradients as they depend on the magnitude of the currents which are not known *a priori*. Thus, 3DD provides a boundary condition, called the “Coriolis Boundary”, which uses the predicted currents to calculate the pressure gradients along the boundary and then applies this information directly back into the water level boundary condition as the model is running. The Coriolis boundary condition has been shown in simulations to be very stable and effective.

For the Bay of Plenty, both boundaries were set up as sea level boundaries, adopting a constant MSL elevation of 1.1 m above Chart Datum. A Coriolis boundary was applied to the northern boundary, with an eastern pivot. That is, the eastern end of the boundary is fixed while the adjustments due to Coriolis force are made successively to cells from east to west along the boundary. In essence, this can be visualised as a flapping water boundary, hinged at the eastern end. Notably, the fixed sea level of 1.1 m on the boundary is the Mean Sea Level (MSL). While 3DD has been used successfully to forecast coastal-trapped wave dynamics, no attempt has been made to incorporate the coastal trapped waves that may be coming around East Cape and affecting the dynamics of the Bay of Plenty in this boundary condition.

To introduce rivers, eight point sources were defined around the Bay (Figure 1.1). In 3DD, the flows are input to the model as a volume flux in the upper reaches of the river. At this stage of the modelling, time series of the daily averages of measured flow rates were adopted in cumecs (m^3s^{-1}).

4.1.1 Wind Measurements

Time series of atmospheric and wind data (January 2003 – December 2004) is available from both Tauranga (-37.673° 176.196°, 4 m height WGS84) and Whakatane airports (-37.926° 176.919°, 7 m height WGS84). These wind records were scaled to a height of 10 m using a logarithmic profile (with roughness length $z_0 = 0.002$ m) and converted to boundary files for 3DD. These are the only two available sites in the grid and so they are both used in the model, which applies an interpolation to all cells, based on the inverse square of the distance from the stations. It is evident that the two stations are different (Figure 4.1) and so spatial variability in wind will need to be accounted for. Consequently with supporting calibration, additional winds were taken from satellite observations over the domain.

Additional wind data has been obtained from < <http://poet.jpl.nasa.gov/> > PODAAC Product #109. The data originated from the QuikScat Scatterometer. The SeaWinds instrument on the QuikSCAT satellite is a specialized radar that measures near-surface wind speed and direction at a 25 km resolution. This instrument was launched on 19 June 1999 and has been measuring winds over approximately 90% the ice-free ocean on a daily basis since 19 July 1999. QuikSCAT is a polar orbiting satellite with an 1800 km wide measurement swath on the earth's surface. Generally, this results in twice per day coverage over a given geographic region. Wind retrievals are done on a 25km x 25 km spatial scale.

Figure 4.2 shows the comparison of Tauranga airport winds and those from QuikScat. While the patterns are close, there are some substantial differences and the magnitudes and duration of events. The QuikScat is seeing a broader spatial average than the anemometer. Calibration of the model is therefore required to determine which winds will be best for predicting the measured currents.

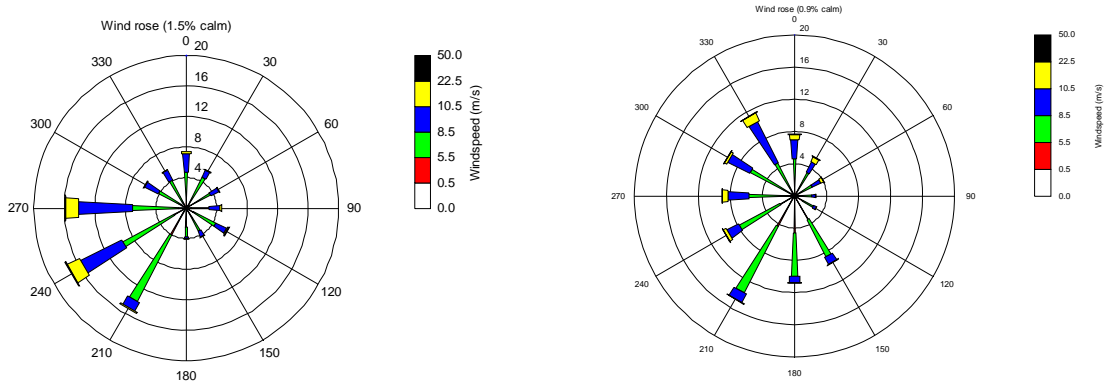


Figure 4.1 - Tauranga (left) and Whakatane (right) wind data from January 2003 to December 2004. Data from anemometers located at Tauranga and Whakatane Airports.

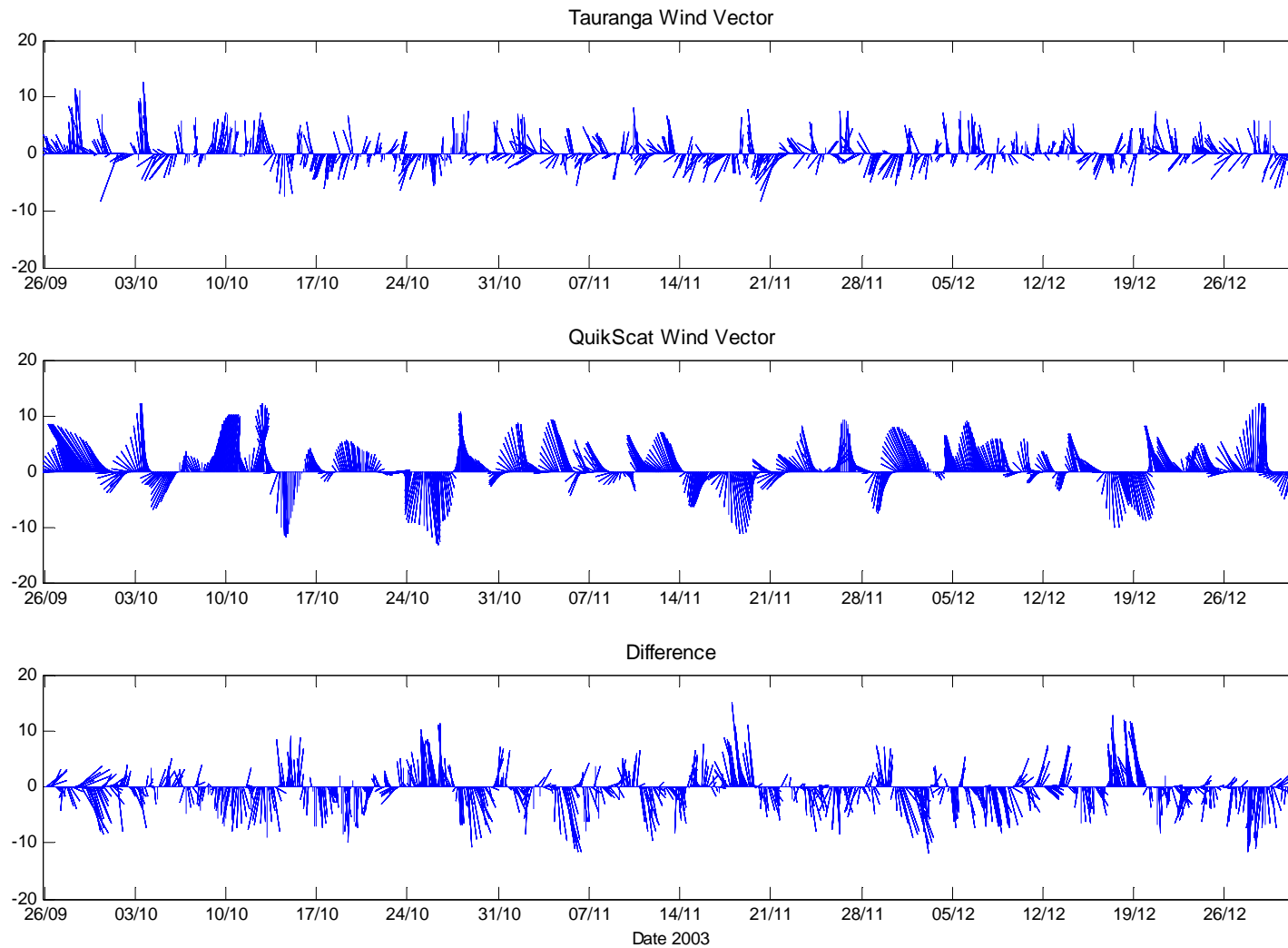


Figure 4.2 – Tauranga airport measured wind velocities, inferred and interpolated QuikScat wind velocities (for a single point closest to Tauranga Airport), and the difference between them.

4.2 Calibration / Validation Data

An Acoustic Doppler Profiler (ADP) was deployed at various sites throughout the Bay of Plenty during 2003 and 2004. Data from one of these deployments offshore from Pukehina (282904 mE, 638317 mN [NZMG1949]) was depth-averaged and processed to remove the tidal signal, as described above. Residual currents at the ADP site were then obtained by removing the tidal signal from the raw data and applied in the model calibration.

4.3 Model Runs

4.3.1 Run 2

4.3.1.1 Details

Initially both the Tauranga and Whakatane Airport winds were used to drive the model. Tests with the 3DD model indicated that these winds needed further scaling to generate the appropriate velocities within the water column and so the winds were scaled by a factor of 1.5 and used to drive the model. The scale factor may account for the difference in wind strength which occurs over land and water.

4.3.1.2 Outcome

As anticipated for a 2D simulation, the model mostly fails to replicate the observed on/offshore currents (Figure 4.3). This occurs because much of the cross-shore movement is due to up/downwelling which cannot be simulated in a single-layer depth-averaged model. In the alongshore direction however, the model replicates several of the southeasterly (positive alongshore) directed flows well. On the contrary, several of the observed northwesterly (negative alongshore) directed flows (~ 8/10, 16/10, 27/10, 8/11) are not being well replicated.

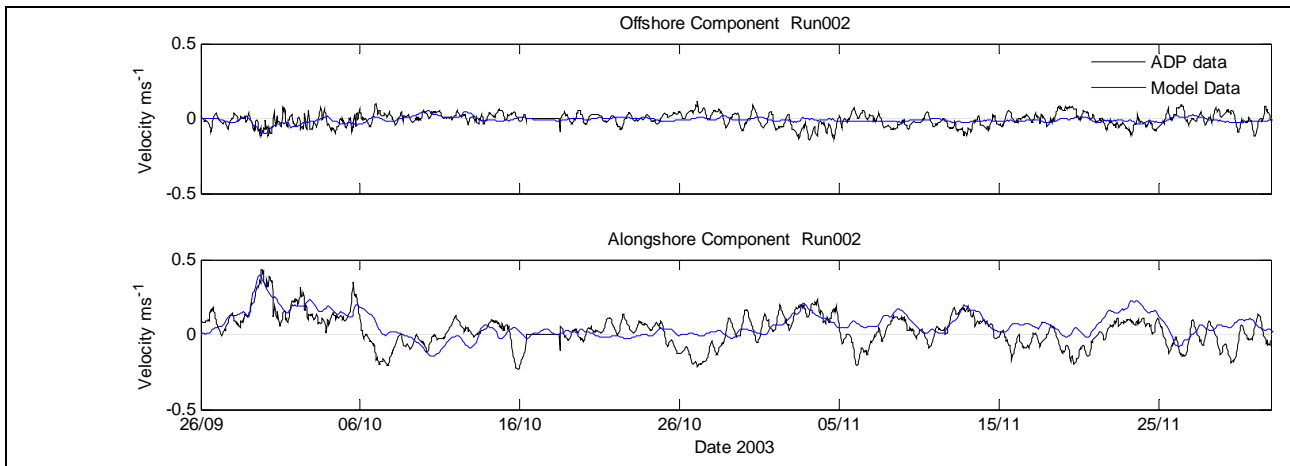


Figure 4.3 - Run 002 results at the Pukehina ADP site. The model was driven with the Tauranga and Whakatane Winds scaled by a factor of 1.5. The offshore and alongshore components are relative to the bathymetry contours and coastline surrounding the ADP site.

Run 7

Details

QuikScat satellite wind data was obtained over the entire grid. A total of 14 wind station points were used to drive the model. The raw data was interpolated using a spline interpolation at 3 hour intervals. The interpolated data set is similar to the wind field measured at Tauranga (Figure 4.4 and 4.5). However, the interpolation scheme and the satellite spatial averaging results in a smoother wind field from the satellites than from the airport anemometers.

Outcome

The model correctly predicts the occurrence of the northwesterly (positive alongshore) flows (Figure 4.5), although the magnitude is often greater than that observed with the ADP indicating that better results may be possible by scaling down the QuikScat winds by a factor. The model shows more movement in the offshore direction and indicates more of a willingness to generate the southeasterly (negative alongshore) flows (~18/11/03 and 27/11/03) that were not present when the model was being driven by the Tauranga and Whakatane airport wind records. However, there are no events in the wind forcing that would fully explain these observed southeasterly flows, which also explains the failure of the 2D model to replicate these events.

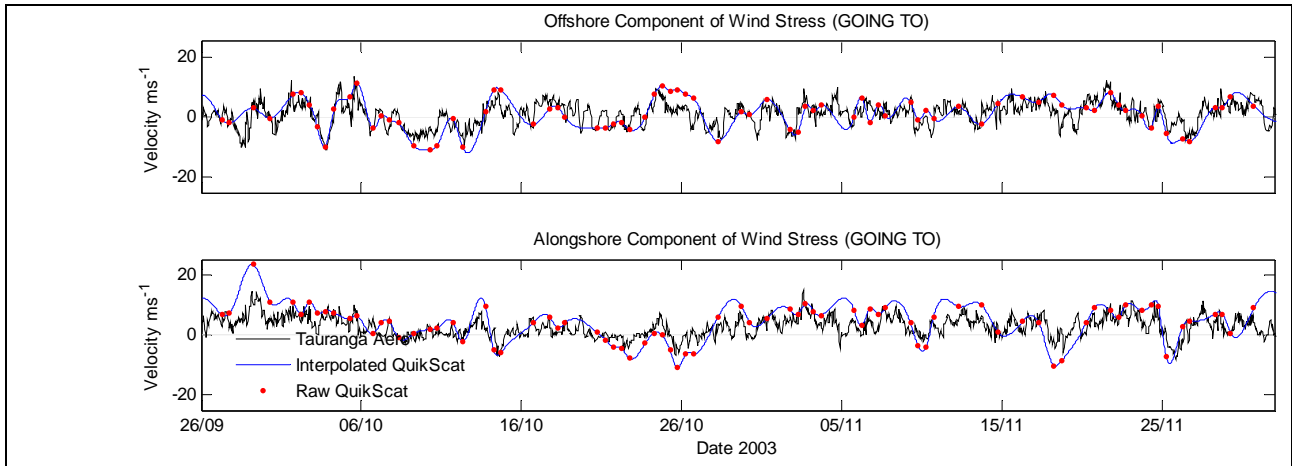


Figure 4.4 – QuikScat wind raw data (red points), 3 hourly splinar interpolated data (blue line) and the Tauranga airport wind records, directions relative to the Pukehina bathymetry and coastline.

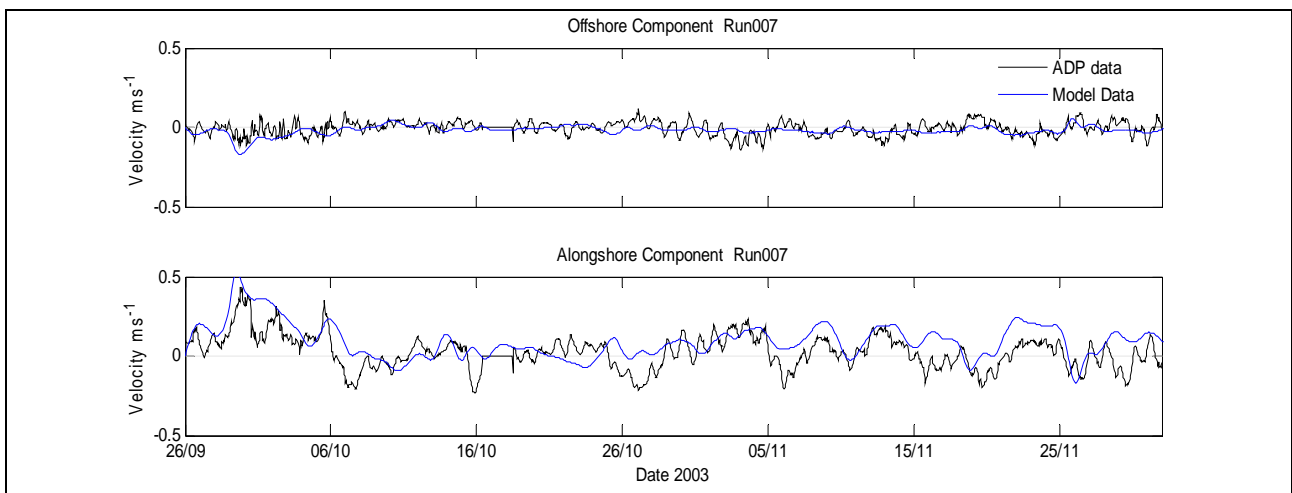


Figure 4.5 – Modelled currents from Run 7 – 14 QuikScat wind stations - and observed water currents from the ADP. Directions relative to the Pukehina bathymetry and coastline.

Run 8

Details

The same 14 QuikScat wind stations from Run 7 were used with a scale factor of 0.8 to reduce the magnitude of the forcing from that used in the previous run.

Outcome

The magnitude of the predicted current oscillations in both the cross-shore and longshore directions is reduced accordingly (Figure 4.6). Given that the modelling in 2D is not able to treat

the cross-shore dynamics and that modelling in 3DHomo and 3DStrat is planned, further calibration is not warranted in the 2D model.

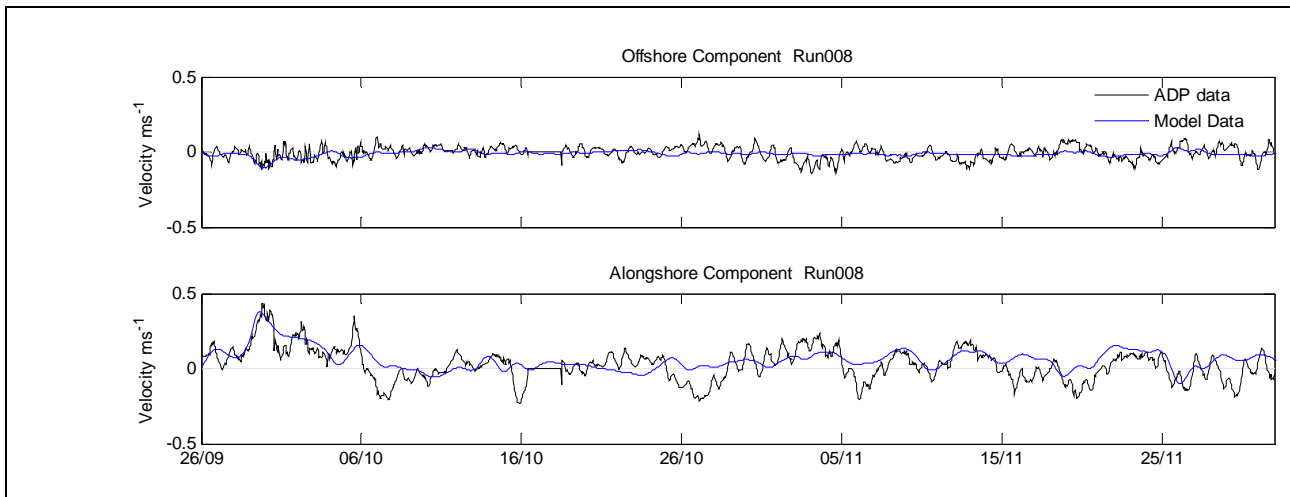


Figure 4.6 – Run008, 14 QuikScat wind stations scaled to 0.8 of their original magnitude.

4.4 Summary of 2D Calibration Runs

The QuikScat winds are more suited to driving the model than the Tauranga and Whakatane Airport data. Possibly, the anemometers recording this data are in fact somewhat sheltered from several wind directions, as a result of the large scale topography of the land e.g. the Kaimai mountain ranges.

The QuikScat winds need to be scaled down by a factor of 0.8-1.0 to generate the appropriate magnitudes of water velocities with the model. However, a final magnitude of the scaling is best left until more of the dynamics of the system is being treated in the 3DStrat modelling.

All model runs failed to replicate several separate periods of observed northwesterly flows (negative alongshore). These flows occurred on approximately 7-8/10/03, 16/10/03, 27-28/10/03 and 20/11/03. The winds used to drive the model (both the measured Tauranga and Whakatane winds and the inferred QuikScat winds) do not display events that are likely to lead to these flows and so they are not explained by wind forcing and cannot be duplicated in the model driven by winds. The currents measured by the ADP at these times should be investigated further to define the nature and potential causes of these flows.

The model fails to replicate accurately the on/offshore flows observed with the ADP, as anticipated for a single-layer depth-averaged model. While mostly effective in the longshore (the 2D model using the QuikScat winds is replicating the wind forced events well), it is apparent that other factors are also forcing the water currents in the area.

4.5 Westerly Currents

Several northwesterly flows (negative alongshore) observed in the ADP data are not being replicated by the 2D model. Investigation of the wind fields surrounding these events indicate that they are not associated with longshore wind stresses (at least those measured at Tauranga, Whakatane or inferred from the QuikScat satellite sensors). Specific times of these events are 7/10/03, 16/10/03, 27/10/03, and 19/11/03.

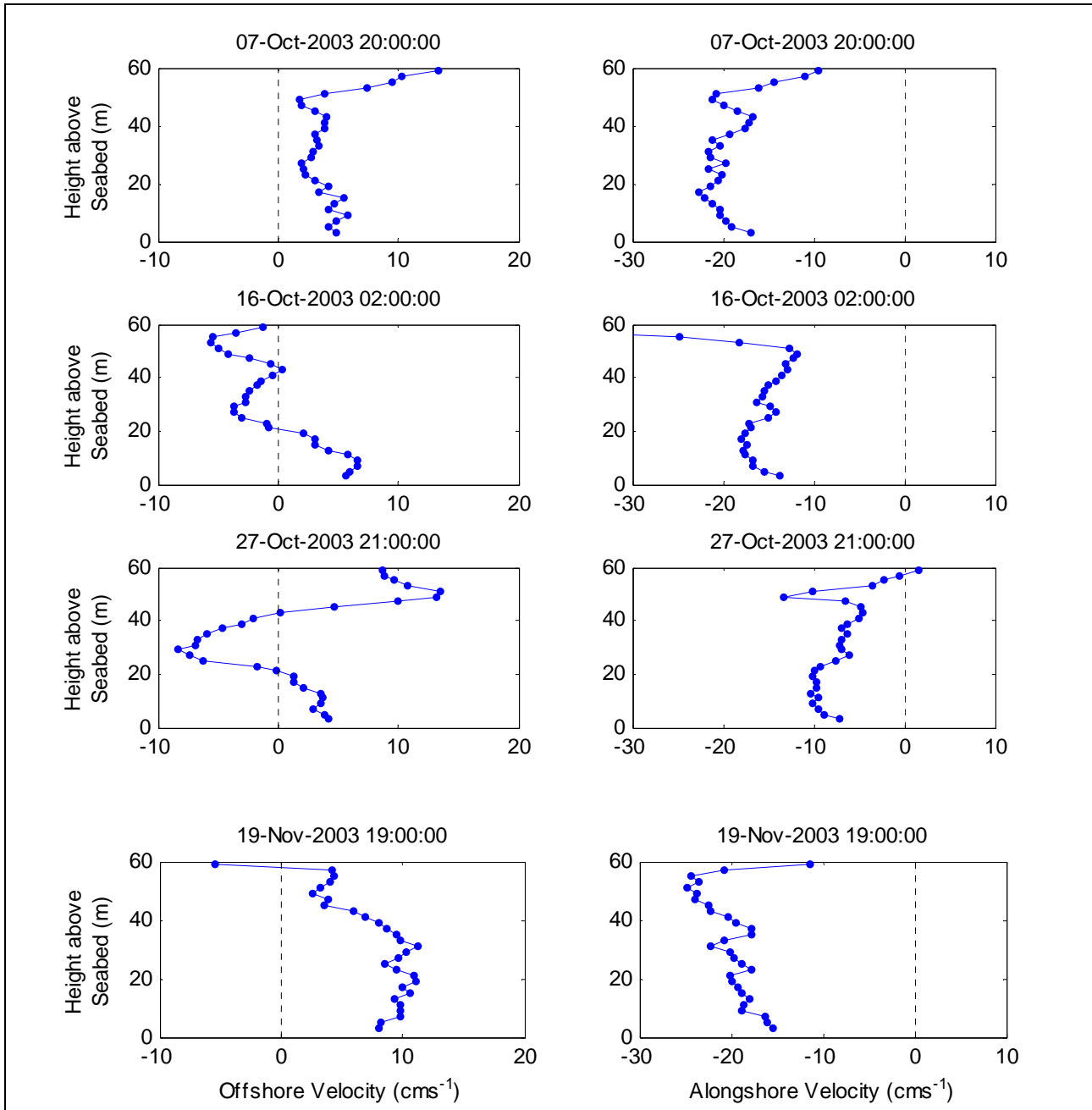


Figure 4.7 – Velocity profiles from ADP current meter during times of depth averaged northwesterly flow. Velocities relative to coastline and bathymetry contours at Pukehina ADP site.

The ADP current profiles at these times (Figure 4.7) indicate variable cross-shore flows. However the direction of the cross-shore flow at the seabed is always positive at depth, indicative of downwelling. Although the surface current appears to be more variable, the bottom currents are consistent with a current travelling north-west along the coast, leading to inshore flow at the surface due to Coriolis and offshore flow at depth (Coriolis-induced downwelling).

The profiles suggest stratification, with the depth of the thermocline generally close to 10-15 m below the surface where the longshore profiles change sharply at this depth, although the depth of the thermocline may be closer to the surface on 19/11.

Measured water temperatures at the ADP site over the calibration period depict 3 weeks from 12/10 to 3/11 when the upper water column became highly temperature stratified with a difference of up to 3°C between the surface layer and the 20 m depth (Figure 4.8). The observed northwesterly flows occurred on 7/10/03, 16/10/03, 27/10/03, and 19/11/03. At these times, stratification is present, but not very strong on the 7/10 and 19/11. As such, full 3DStrat modelling is needed to determine the effects of the stratification on the flows.

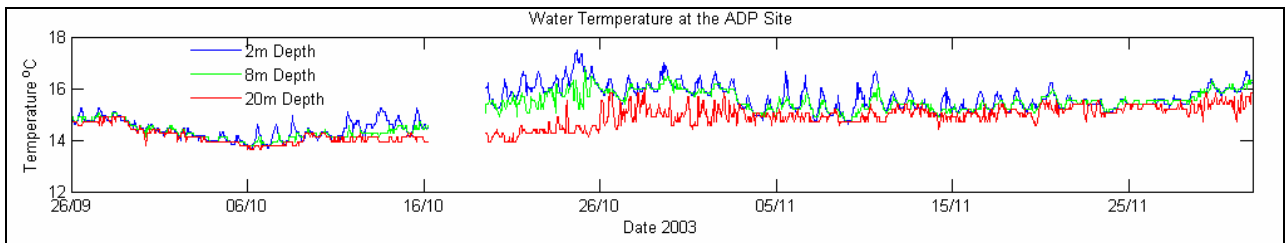


Figure 4.8– Water temperatures at the Pukehina ADP site for the calibration period. Temperatures measured by TidBit® Stowaway temperature sensors. Missing data is due to servicing of the temperature string.

5 3D Homogenous Model Runs

In the next stage of modelling, 3DHomo (barotropic) simulations were undertaken. In these, the model is broken into a series of vertical layers, and the equations are solved in each layer and linked by vertical eddy viscosity. This allows the model to discriminate currents with depth in the water column. Ten layers were adopted and the chosen layer thicknesses are shown in table 5.1 and 5.2.

Table 5.1 The 10 layers used in the 3DHomo simulations

Layer Number	Layer thickness	Depth at bottom of layer
1	5	5
2	10	15
3	10	25
4	10	35
5	15	50
6	20	70
7	40	110
8	100	210
9	400	250
10	1500	1725

Table 5.2 The 10 layers used in the 3DStrat simulations, with different layer interface positions to allow better representation of the temperature structure.

1	5
2	10
3	10
4	10
5	15
6	20
7	80
8	100
9	250
10	500

To simplify user operation, the 3DD Suite uses with the same input files and boundary files as the 2D case and so all inputs and model calibration coefficients remain the same as those described above for the 2D modelling.

The model shows good and improved replication of the measured current velocities (Figure 5.1 and 5.2). We have used the parabolic formula (eqn 18) in Model 3DD to specify the vertical eddy viscosity which links the layers. As this formula is fully determined by the model, no calibration of vertical eddy viscosity is possible. As such, the 3DHomo model has only 2 calibration factors (friction and horizontal eddy viscosity) which is the same as the 2D model and the same values were adopted in the 3D model. Boundary conditions and other inputs are also the same. Thus, the improved calibration must be due to the ability of the 3DHomo model to discriminate in the vertical. Thus, further improvement may be anticipated when stratification is represented in the model.

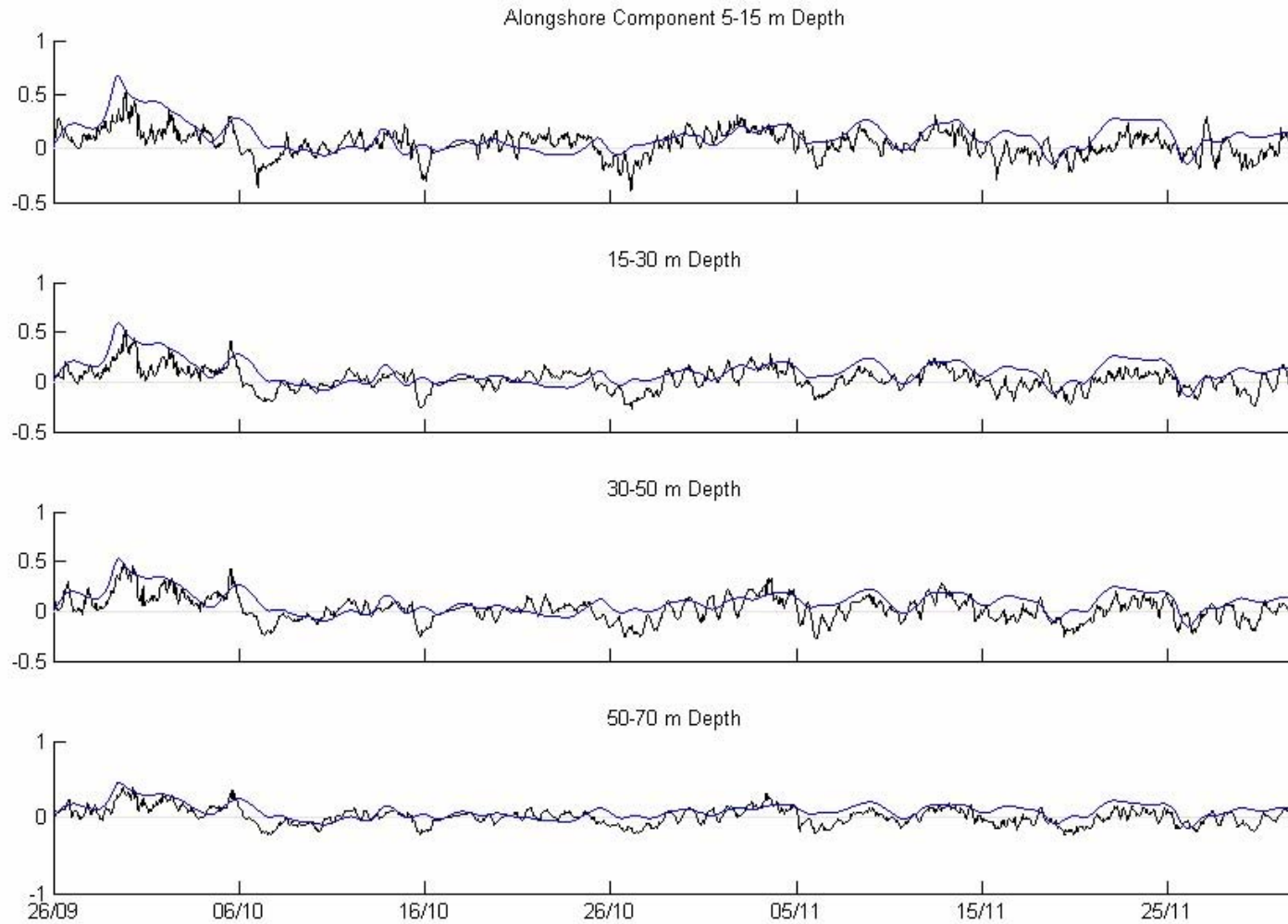


Figure 5.1- Alongshore component of measured and modelled velocities Model is the smoother blue line.

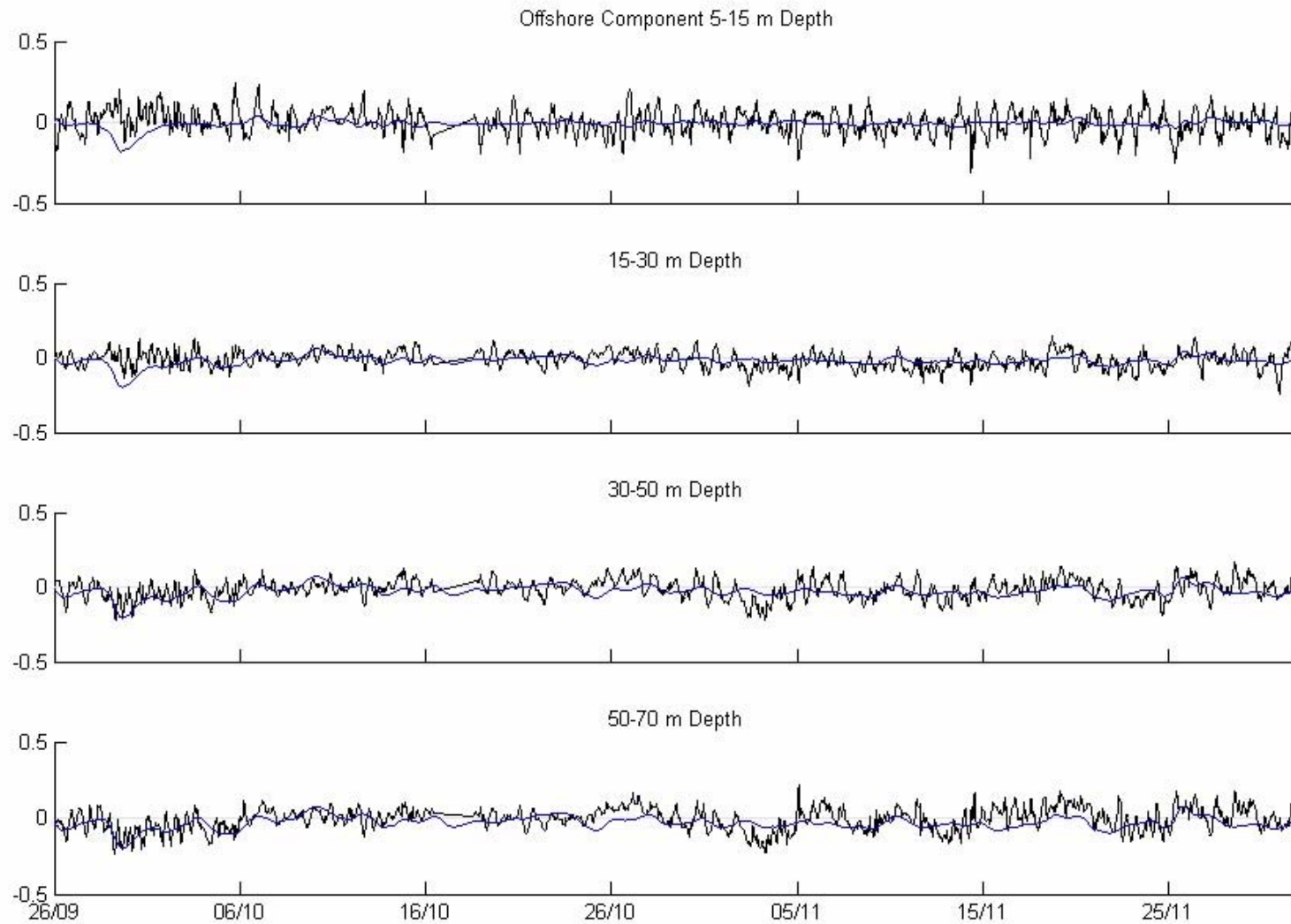


Figure 5.2 - Offshore component of measured and modelled current velocities. Model is the smoother blue line.

6 3D BAROCLINIC MODEL RUNS

6.1 Specifying Temperature and Salinity across the grid

Several new inputs are needed for the 3D baroclinic modelling. First, an “initial condition” is required to specify velocity, temperature and salinity within the Bay at all cells at the start of the run. Specialist software was developed for this purpose and incorporated into the 3DD Suite with the chosen values placed in a “hot start” file which transfers the gridded values to the model at the beginning of the run. Sites where data was recorded are shown in Table 6.1.

Table 6.1 Data collection sites. The columns 3k_i and 3k_j give the I and J coordinates of the sites in the 3 km grid.

Transect	ID	depth	NZMGx	NZMGy	DFS	3k_i	3k_j
Pukehina	AAP10	10m	2827892	6369054	844.52	23.2973	10.018
Pukehina	AAP20	20m	2828533	6370066	2042.45	23.511	10.3553
Pukehina	AAP30	30m	2830408	6373078	5590.34	24.136	11.3593
Pukehina	AAP50	50m	2832774	6376884	10071.79	24.9247	12.628
Pukehina	AAP100	100m	2838278	6385687	20453.83	26.7593	15.5623
Pukehina	AAP200	200m	2840189	6388745	24059.84	27.3963	16.5817
Whakatane	AAW10	10m	2862981	6355319	1119.92	34.9937	5.4397
Whakatane	AAW20	20m	2863604	6356112	2120.23	35.2013	5.704
Whakatane	AAW30	30m	2865348	6359499	5923.3	35.7827	6.833
Whakatane	AAW50	50m	2867899	6363124	10342.59	36.633	8.0413
Whakatane	AAW100	100m	2875140	6376649	25671.71	39.0467	12.5497
Whakatane	AAW200	200m	2877580	6380890	30564.48	39.86	13.9633
Opotiki	AAO10	10m	2884479	6349415	1458.46	42.1597	3.4717
Opotiki	AAO20	20m	2884636	6350990	3041.15	42.212	3.9967
Opotiki	AAO30	30m	2885047	6354233	6309.83	42.349	5.0777
Opotiki	AAO50	50m	2886021	6361859	13997.62	42.6737	7.6197
Opotiki	AAO100	100m	2887710	6375147	27392.48	43.2367	12.049
Opotiki	AAO200	200m	2888933	6384817	37139.5	43.6443	15.2723

CTD data was recorded along the cross-shore transects on 17/10/2003, 03/12/2003, 18/03/2004, 08/04/2004, 25/5/2004, 01/08/2004, and 08/12/2004. As the CTD data set obtained on 17/10/2004 was the closest (22 days) to that of the start of the calibration period on 26 September 2003, it was used for the initial conditions in the depth range of the measurement sites.

The measurements are restricted to less than 200 m water depth and other inputs are required to specify conditions at deeper locations in the grid. For simplicity and because the deeper areas are not of primary interest to the study, all depths greater than 1000 m in the grid were truncated to 1000 m.

To set the offshore values, several datasets were combined, including:

- Sutton and Roemmich (2001)
- XBT surveys from the Global Temperature-Salinity Profile Program for September 2003. http://www.nodc.noaa.gov/cgi-bin/GTSPP/gtspp_action.cgi. The Global Temperature-Salinity Profile Program (GTSPP) is a cooperative international program designed to develop and maintain a global ocean T-S resource with data that are as up-to-date and of the highest quality as possible. The primary goal of the GTSPP is to make these data quickly and easily accessible to users.
- Combined OSD, CTD, XBT, PFL measurements from <http://www.nodc.noaa.gov/cgi-bin/OC5/SELECT/dbextract.pl> between 1978-1992.

Figure 6.1 shows the 19755 stations where measurements were made during September 2003 in the global oceans, including the Bay of Plenty region. The locations of the combined OSD, CTD, XBT and PFL measurement locations are shown in Figure 6.2.

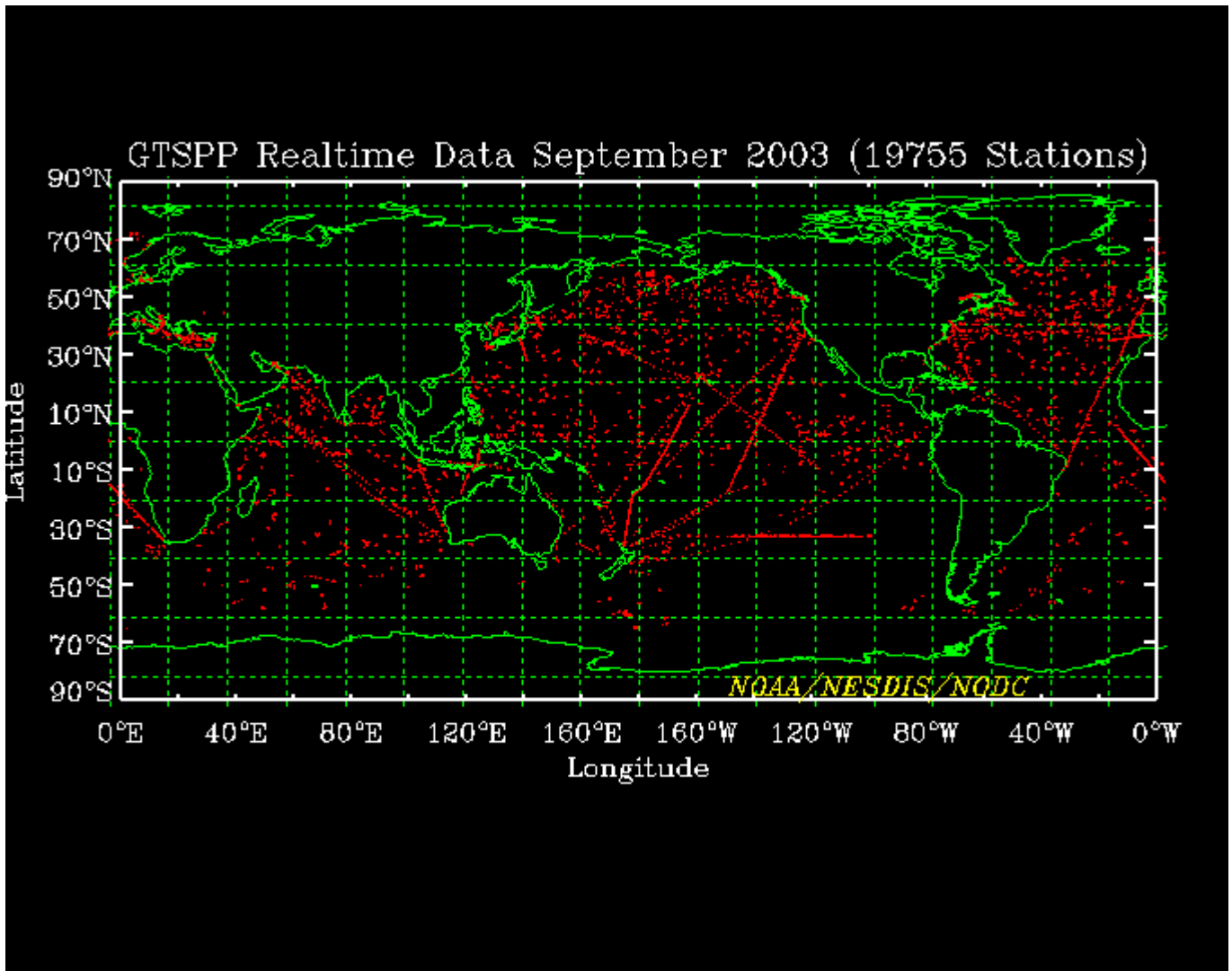


Figure 6.1 - Locations of measurements in September 2003.

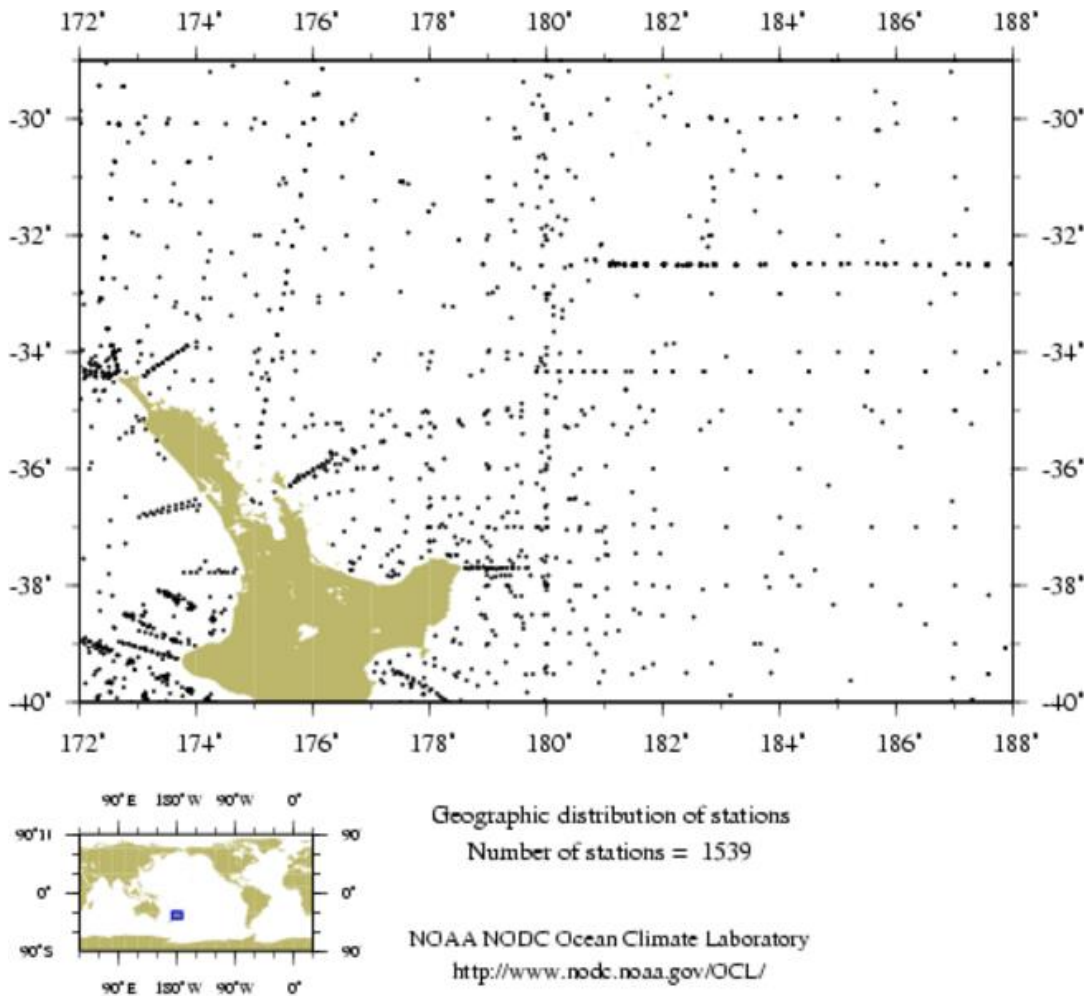


Figure 6.2- Combined OSD,CTD,XBT,PFL measurements from <http://www.nodc.noaa.gov/cgi-bin/OC5/SELECT/dbextract.pl>.

The values from the CTD cast are used near the shoreline. To prevent linear extrapolation techniques from exaggerating the values of the salinity and temperature at the boundaries of the grid, a few points were required to be defined at the oceanic extent of the grid. For these data, two XBT profiles (from 2003/09/08 and 2003/09/13) were averaged for the temperature data, and CTD casts from a variety of dates were averaged for the salinity profiles. It was found that the profiles varied seasonally and the depth of the thermocline increased slowly from October to April and then rose sharply as the cooling winter season commenced (Figure 6.3 and 6.4).

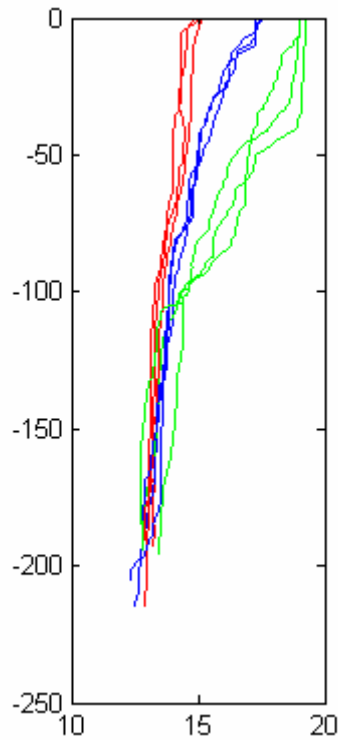


Figure 6.3– Typical profiles of temperature within the Bay of Plenty during the year. Green lines are summer time measurements, blue lines are spring and autumn measurements and red lines are winter measurements.

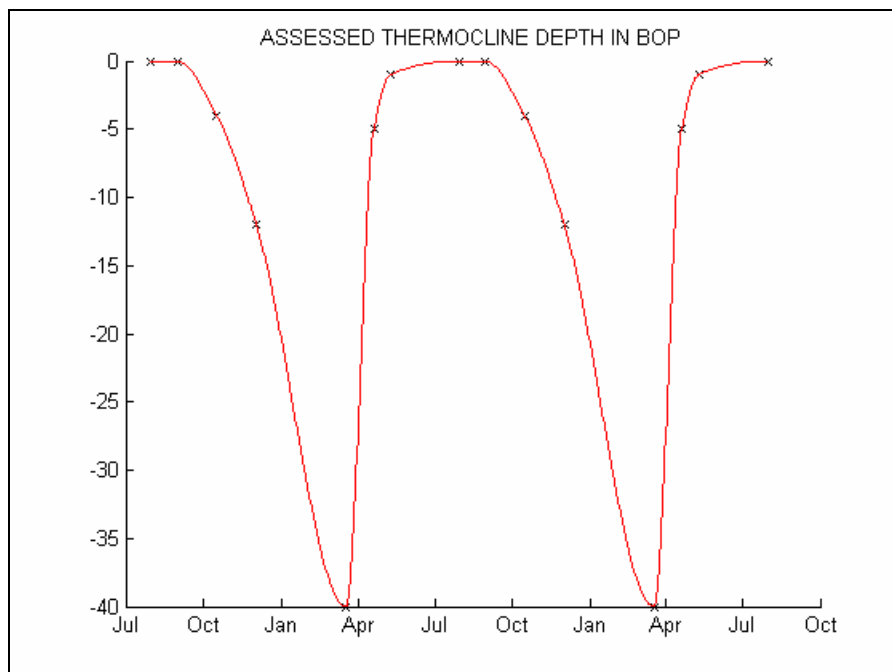


Figure 6.4 – Assessed thermocline depth in the Bay of Plenty from numerous CTD casts over time.

For the surface layer of the model, we adopted the temperatures from the satellite sea surface temperatures recorded at the model start time. The data was interpolated onto the model grid and

smoothed. By using the measured satellite temperatures, the model incorporates the elevated temperatures associated with the warm East Auckland current that penetrates into Bay of Plenty and the highly variable temperatures associated with shallow water heating/cooling and the upwelling that is common around East Cape (Figure 6.5). The satellite images reveal the complexity of the temperature structure in the Bay which is captured by assimilating the satellite data directly into the model.

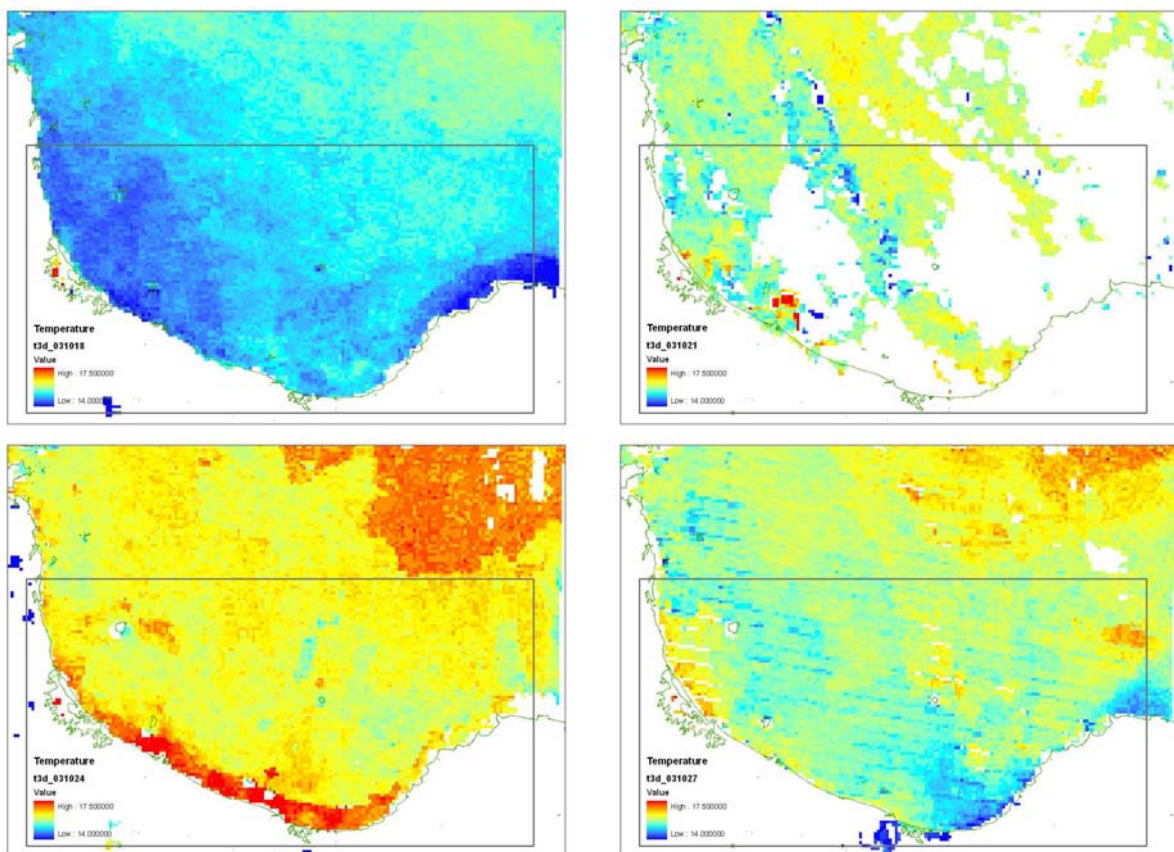


Figure 6.5 - Temperatures recorded by satellite over a period of rapid warming. The plots show temperatures at 3 day intervals starting from October 18, 2004. Other features are the large variations that occur in shallow water near the coast and the upwelling along and around the tip of East Cape.

The light decay constants determining solar heat penetration were obtained by developing a 1-dimensional Matlab model of the heat exchanges and forecasting the measured stratification. This involved utilising the actual measured currents through the water column from the ADP to determine the vertical shear and mixing, which eliminates errors associated with forecasting currents and thereby puts the focus of the model on the ocean/atmosphere heat exchanges. When calibrated against the CTD data, the most appropriate extinction coefficients were found to be $K_L = 0.574$ for the longwavelengths and $K_s = 0.128$ for the short wavelengths. The ratio of long to short wavelengths in the measured solar radiation (PAR) was taken to be 0.75.

6.2 Initial Results

Initial results from the 3DStrat model are shown in Figures 6.6 to 6.9. In these initial runs, the heat equations were adopted without the application of the assimilated satellite temperatures.

In general, the modelled currents replicate the measured currents accurately (Figure 6.6 and Figure 6.7). There is however a discrepancy between 16/10/2003 and 30/10/2003, where the model exaggerates relative to the observations.

In this simulation, standard heat equations were adopted. During calibration, the input solar radiation values were multiplied by 2.6 to maintain temperature within the water column. Such a large multiplier cannot be physically justified and so further calibration is required. Despite this multiplier, the model-predicted temperatures still drift with the model rapidly losing heat from the water column, beginning around 24/10/2003 or ~672 hours into the model run (Figure 6.8). Some of this drift is also due to inaccurate specification of river water temperatures as the salinity plots (Figure 6.9) show salinity reductions due to river water penetration at the calibration site. Eventually, the river temperatures were set to match the satellite temperatures at the entrances of each.

Salinities in the model are very similar to the measured data in layers 2 and 3 (Figure 25). However, the salinities in layer 1 are much lower than the observed values. It is evident that the salinities being applied in the rivers are too low. This occurs because the mixing of ocean and

freshwater which occurs in the lower reaches of the river is not being accounted for. As such, the salinity boundary condition needs to be adjusted for this process by increasing the river salinity. It is not reasonable to adjust the river flow rates as the model is using measured values as time series.

As there are sub-diurnal variations in the offshore component in the velocity which are not expected to be replicated in the QuikScat winds being used to drive the model, the measured data was next smoothed to compare to the model results. These sub-diurnal variations may be due to wave effects, sea breezes or some other influence. With relatively low velocities and rapid changes, these are not expected to be significant with respect to a nutrient dynamics model.

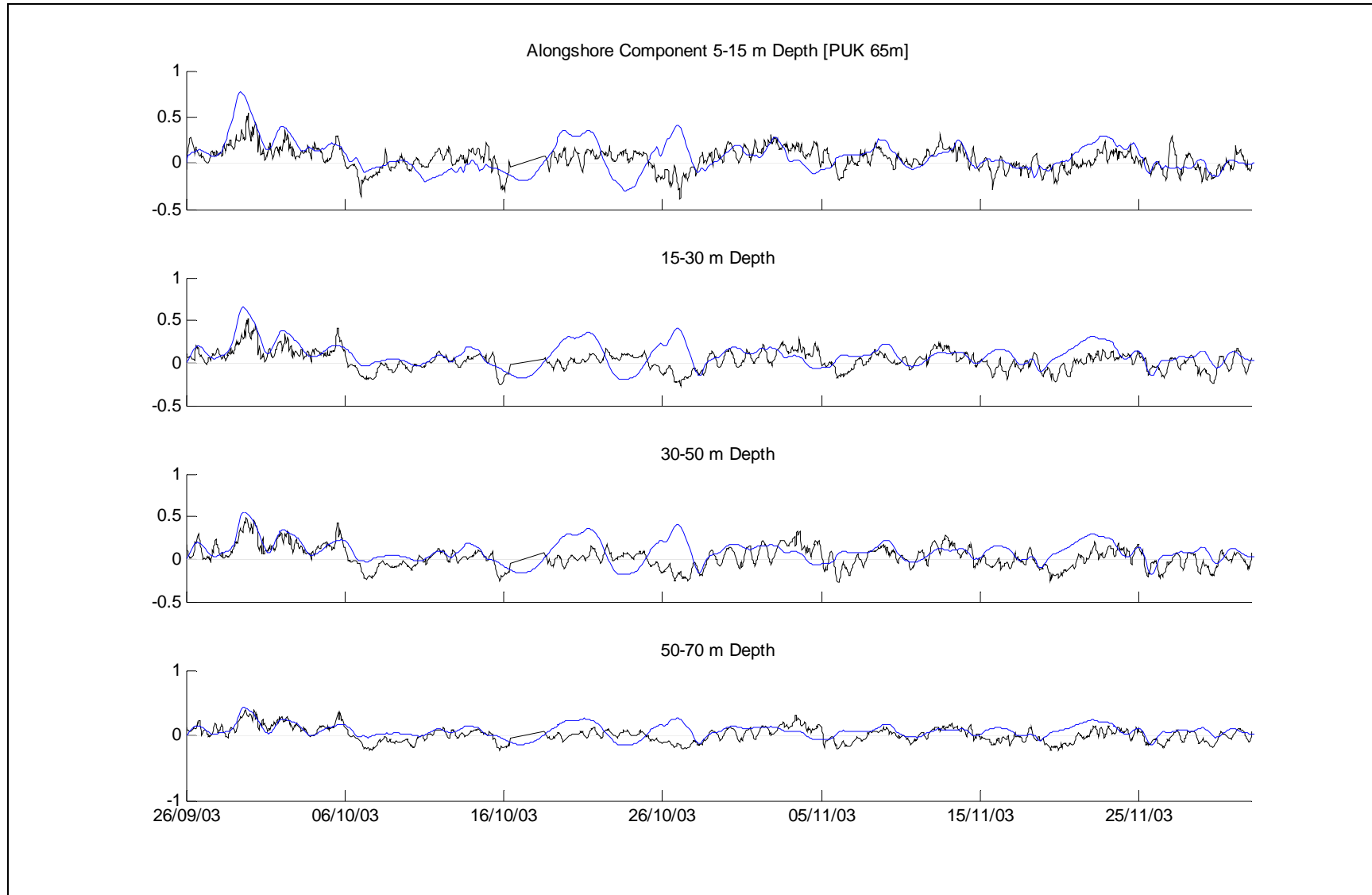


Figure 6.6 - Alongshore model results from Run007

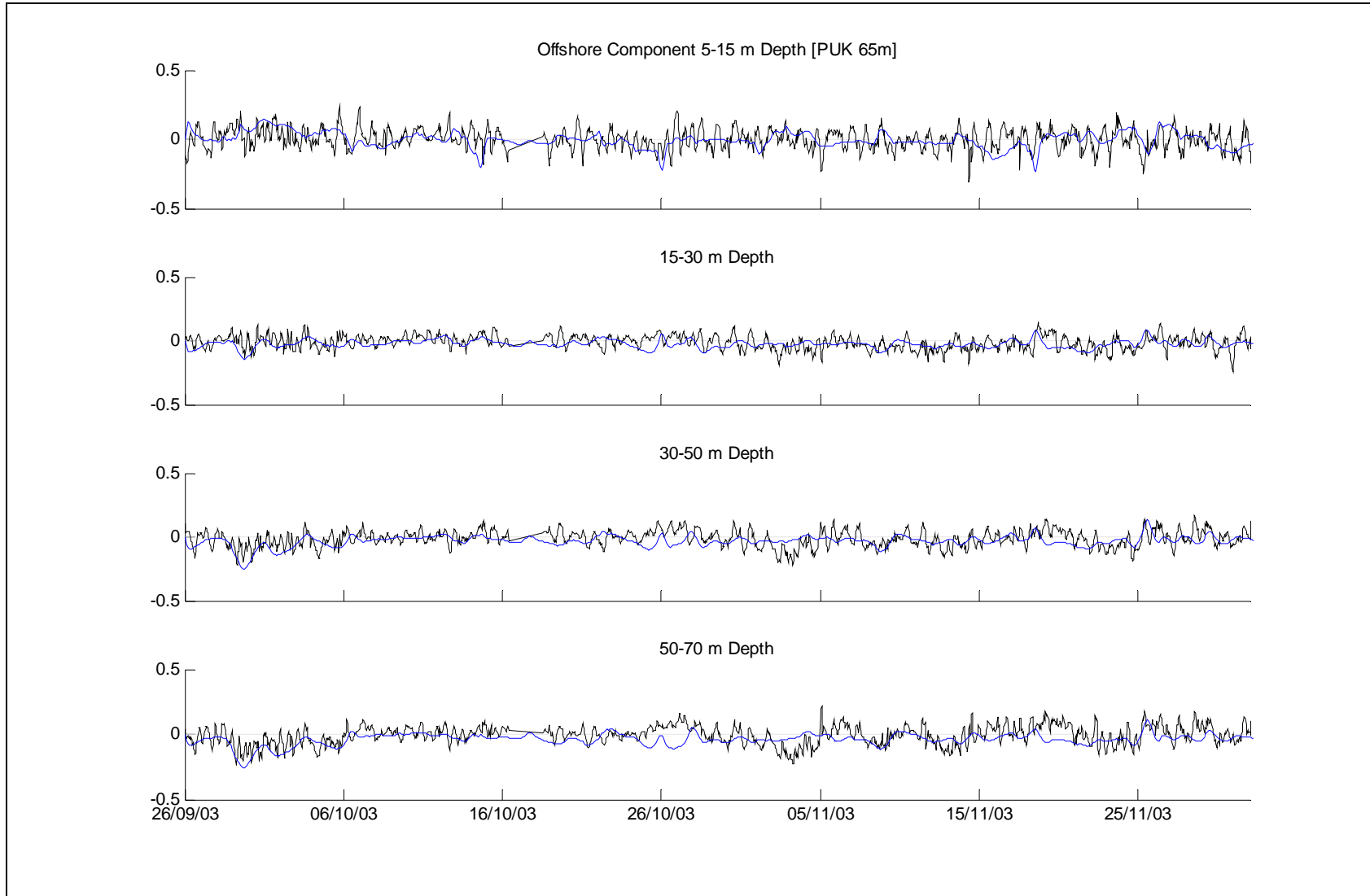


Figure 6.7– On/offshore current velocities from Run007

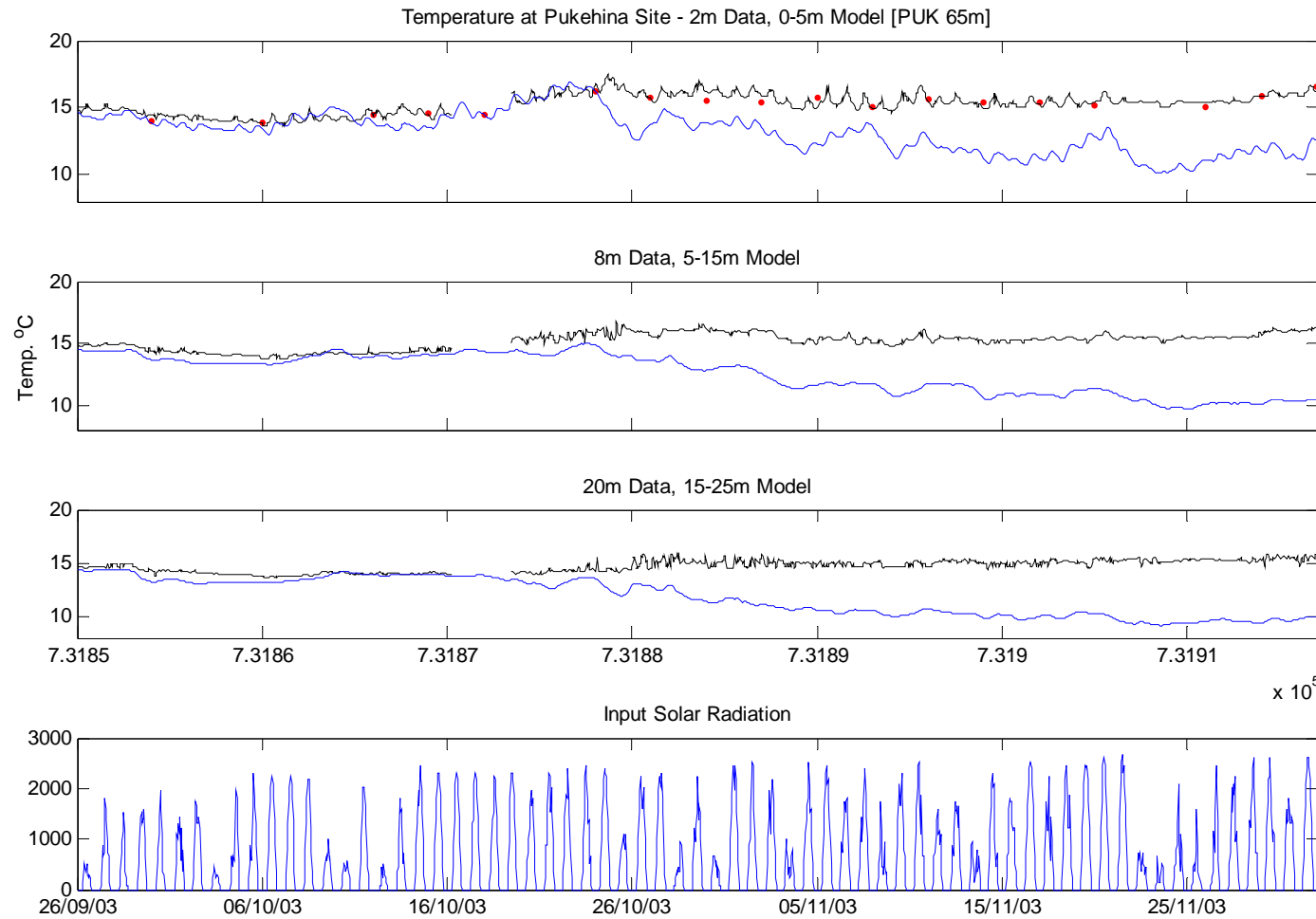


Figure 6.8 - Temperatures from Run007. The red plotted points are the measured temperatures from the data collection programme, which show good correlation with the satellite observations (black line). The model (blue line) drifts and cools without assimilating the satellite data in the model.

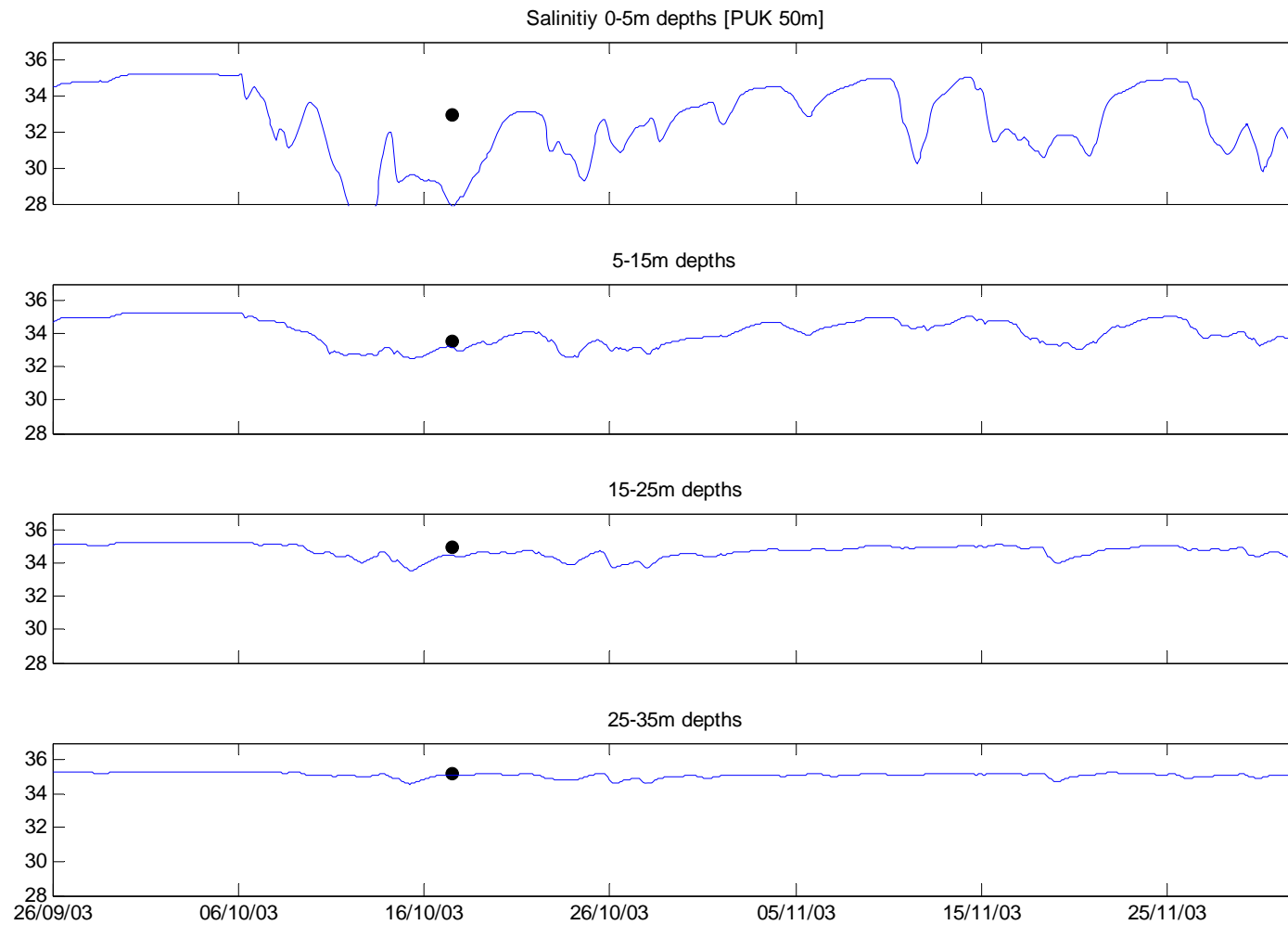


Figure 6.9 - Salinities from Run007 with the recorded data at the Pukehina 50 m deep site. Salinity in the model is too low in the surface layers.

6.3 Run008

In further sensitivity simulations, the solar radiation multiplication factor was reduced to 1.0, river salinities increased and river temperatures were changed to be equal to the 5-day average of the air temperatures minus 1 degree, while the eddy diffusivity was increased to $100 \text{ m}^2\text{s}^{-1}$. Results indicated that the increased salinity and horizontal eddy diffusivity of the model reduced the stratification of the upper few layers and resulted in the elimination of the problem observed with the modelled currents between 16/10/2003 and 30/10/2003. This test confirms the high level of complexity inherent in 3DStrat models and the ‘feedback’ that occurs between density, salinity, temperature, stratification and wind generated currents. The increased salinity of the rivers has resulted in a slightly better comparison between the modelled and measured salinities.

The model temperatures were still drifting and further tests showed that the cause related to two factors:

- Temperature boundary conditions during inflowing conditions were allowing colder water to enter the grid. This was corrected by using the satellite images to set the boundaries at the surface and the initial condition profiles (Figures 6.4 and 6.5) to set the lower levels.
- The heat equations consist of several large magnitude terms and the small difference between these terms can cause drift if there are errors in any of the input values such as wind, relative humidity, barometric pressure etc. This was corrected by applying the novel “nudging” scheme described above, whereby the satellite-sensed temperatures throughout the entire model run were interpolated onto the grid and applied to the 2 upper layers of the model approximately every 3 days. The full heat equations were still embedded in the model and were being used to allow heat penetration from solar radiation. The nudging simply “put the model back on track” every three days and accounted for the complex temperature structure in the Bay. The stability of the model remained excellent with this scheme, even though the 3-day nudges created some minor changes to the temperature fields each time they were imposed.

Further testing considered the long and short wavelength decay coefficients, including changing them from their mean values of 0.574 and 0.128, to the median values of 0.3694 and 0.129 (Table

6.2). However, in the final calibrated simulations, the coefficients were found to be best set to the mean values of 0.57 and 0.13.

Calibration also showed that vertical eddy diffusivity was best set to a very low value of $0.0007 \text{ m}^2\text{s}^{-1}$, due to the Eulerian scheme of the model being vertically diffusive by nature. Notably, values of 0.0001-0.001 are common in deep ocean models and so our calibrated value is compatible with those precedents.

To better represent the cross-shelf sea gradients due to the Coriolis effect, the Coriolis boundary condition described above was adopted on both the north and east bounds of the model, rather than just the north bound. This change is in accordance with the expectation that both boundaries would be affected similarly by the Coriolis force.

Table 6.2 Best fit values of K_L (K_L) and K_S (K_S) for the measured profiles, obtained using the 1-d model. The measurement sites are identified as OPO: Opotiki, PUK: Pukehina, WHK: Whakatane and the depth at the site.

Site	Date	K_L	K_S	R2
OPO 20	3/12/2003	1.362658	0.189479	0.0009
OPO 20	8/04/2004	0.256572	0.199945	0.090043
OPO 20	17/10/2003	0.719332	0.2	0.101755
OPO 20	25/05/2004	0.291137	0.15858	0.024472
OPO 30	3/12/2003	0.460696	0.133816	0.01331
OPO 50	3/12/2003	1.34227	0.125619	0.01229
OPO 50	8/04/2004	0.2	0.095407	0.037892
OPO 100	3/12/2003	0.624608	0.096463	0.014558
OPO 200	3/12/2003	0.447761	0.052304	0.098846
PUK 100	8/04/2004	0.2	0.051572	0.140235
PUK 100	26/05/2004	0.200001	0.060911	0.011835
WHK 10	4/12/2003	1.999766	0.199973	0.017172
WHK 10	17/03/2004	0.735285	0.068001	0.01655
WHK 20	4/12/2003	0.684425	0.167079	0.022277
WHK 20	8/04/2004	0.221262	0.196834	0.069427
WHK 20	17/03/2004	0.2	0.085047	0.020959
WHK 30	17/03/2004	0.2	0.027423	0.077393
WHK 30	17/10/2003	0.276216	0.132401	0.004224
WHK 50	17/10/2003	0.849662	0.199974	0.003175
WHK 50	24/05/2004	0.214598	0.119651	0.02347

River salinity was set to 17 ppt, which is physically reasonable given the amount of tidally-induced mixing that occurs around the entrance of the rivers and in the adjacent inner shelf waters.

Average cloud cover (a variable not measured) was set to 0.45 and input solar radiation is taken as measured without a multiplier (i.e. not scaled). The albedo was set to 0.08.

The final calibration results are shown in Figures 6.10-6.14. We find that the model is effectively reproducing the dynamics of the Bay of Plenty, including both the longshore and cross-shore currents throughout the water column. The salinities and temperatures are closely matching the field measurements. Figure 6.14 shows the spatial distribution of surface salinities and the match with data is very good, indicating that the model inputs, settings and methods (including the horizontal eddy diffusivity) are providing an accurate reproduction of the river impacts on the continental shelf.

Given the complexity of the environment, the results are very encouraging and a tribute to the effort taken over the calibration and the capacity of the model to treat a broad range of processes simultaneously. Numerous other datasets have been considered including a validation of the model against data from a later stage of the field measurement program (Longdill, PhD Univ. Waikato, in prep). The results proved to be very similar to those presented here.

Future work would involve further comparisons with the very broad field dataset, including modelling over longer time periods, with detailed consideration of continental shelf waves and the East Auckland current. Incorporation of these two phenomena would be expected to lead to further improvements in the model calibration.

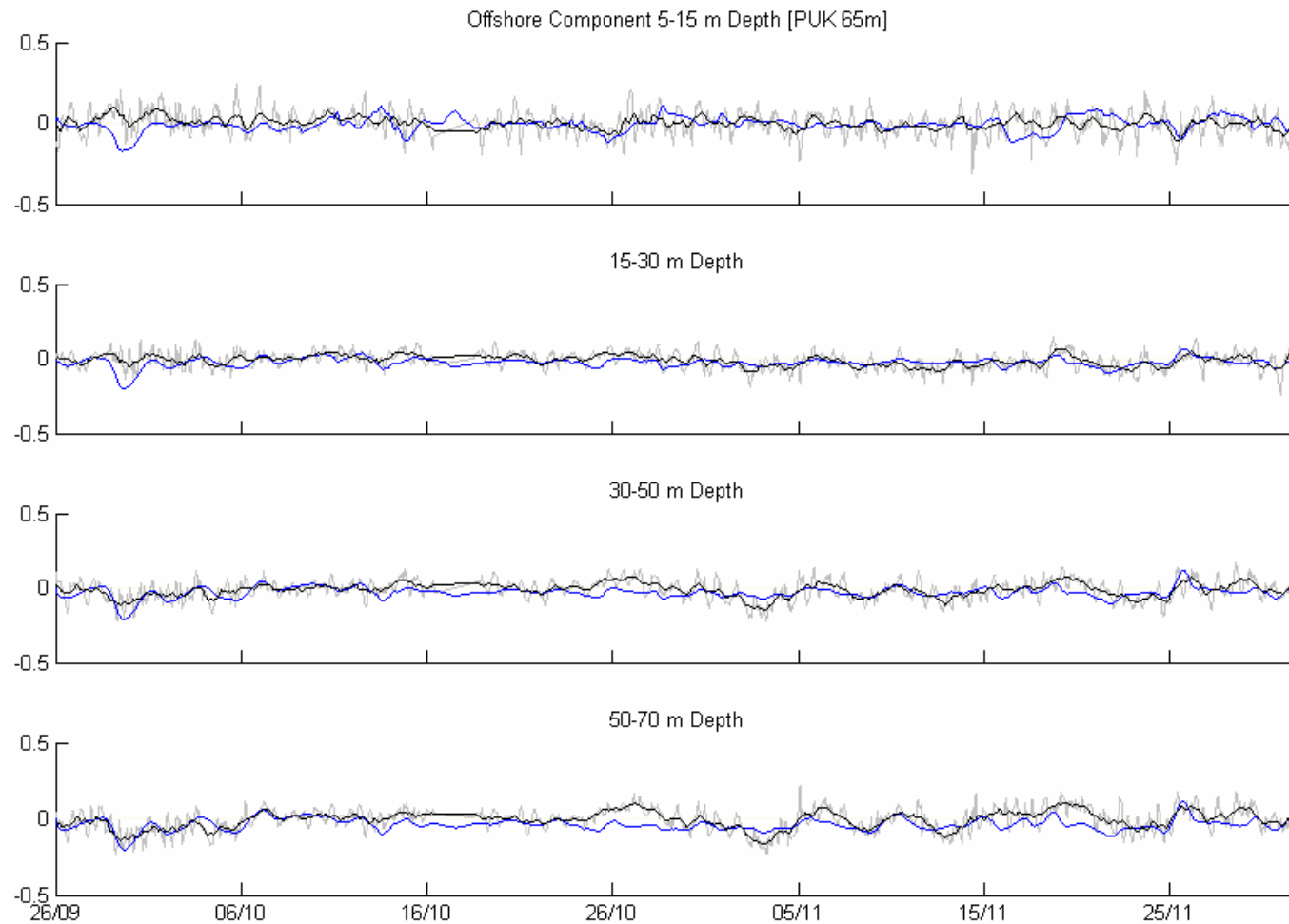


Figure 6.10 – Measured (black line) and modelled (blue line) offshore component of velocity at the Pukehina 50m site. The measured data has been filtered with a running mean filter with a window of 12 hours to reduce short term oscillations in the on-offshore flow. These short term oscillations are thought to be due to wave action or some other forcing which is not incorporated into the present model.

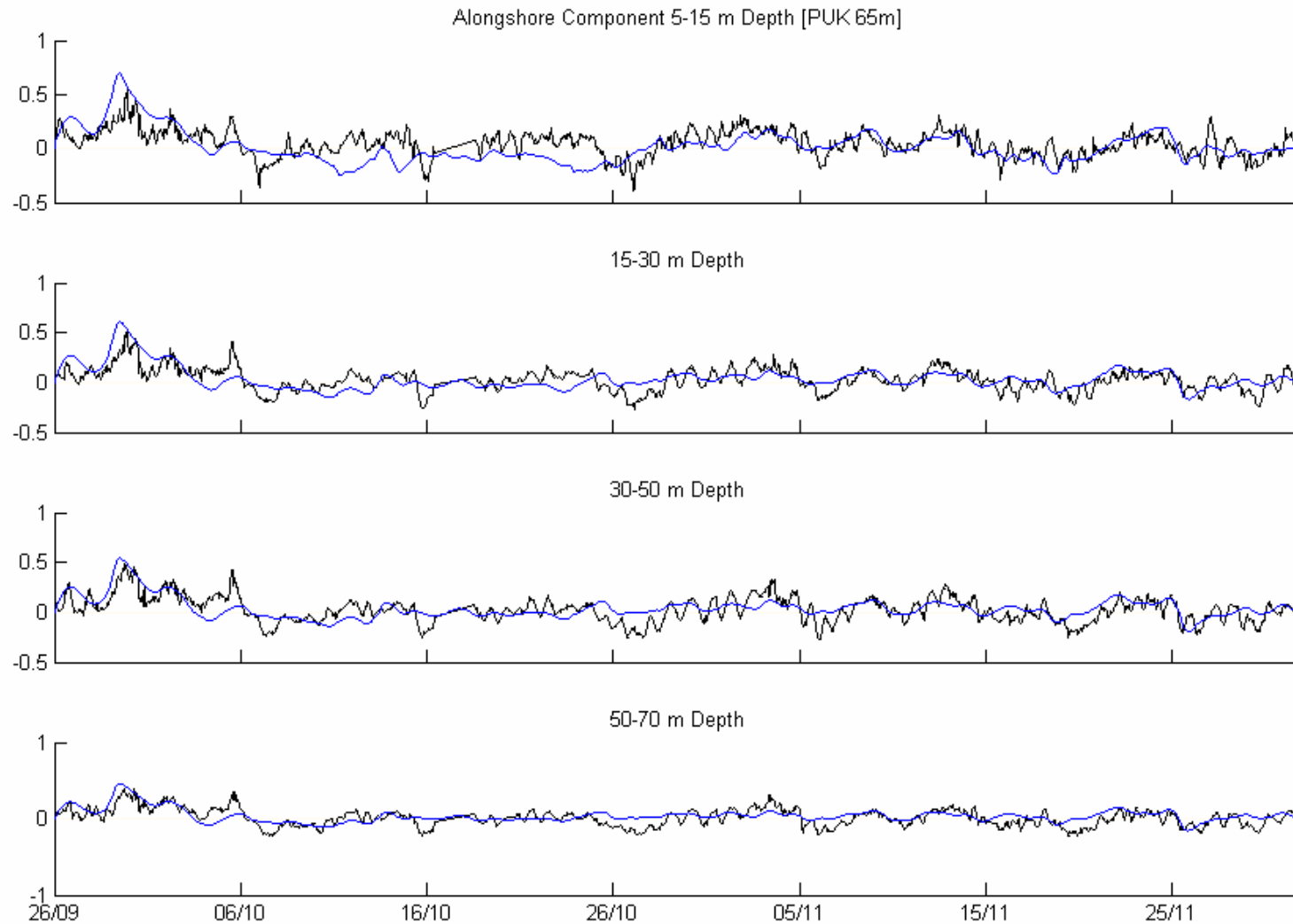


Figure 6.11 – Measured (black line) and modelled (blue line) alongshore component of velocity at the Pukehina 50 m site in the Bay of Plenty.

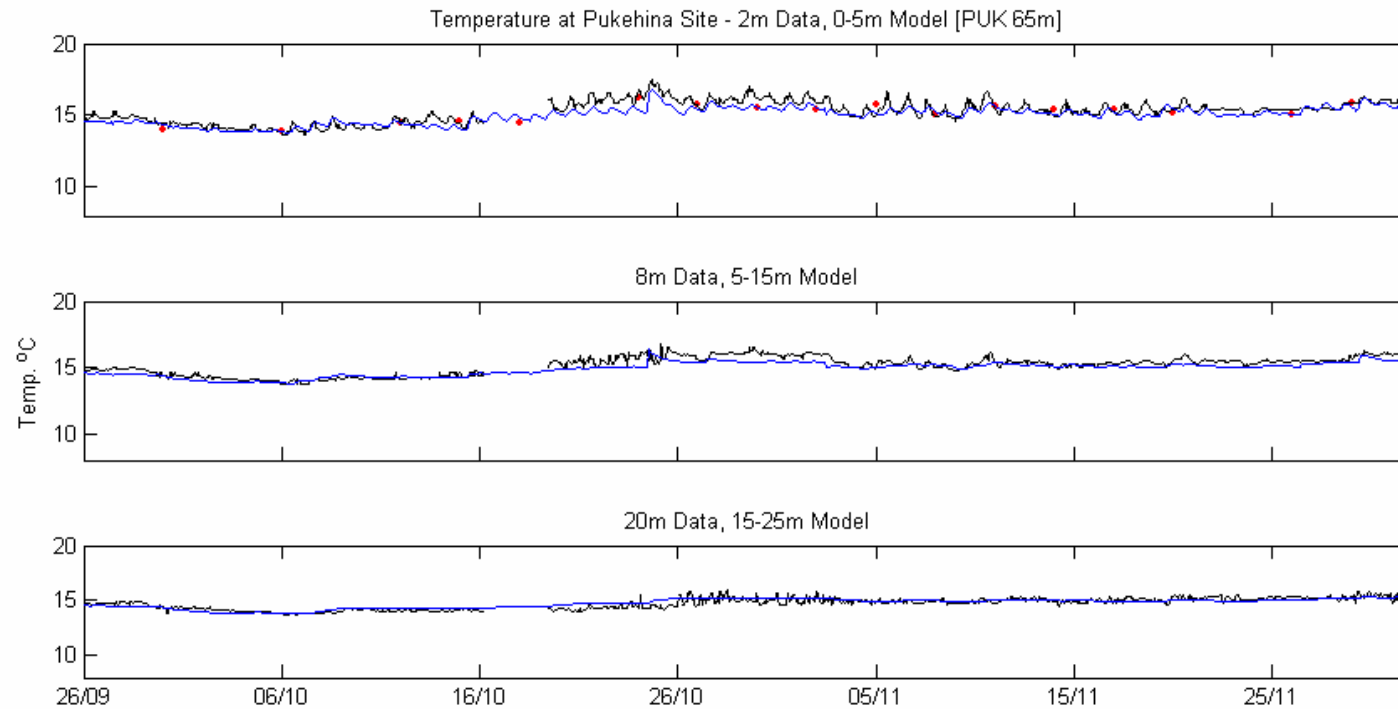


Figure 6.12 – Measured (black line) and modelled temperatures at the Pukehina 65m site. AVHRR Sea Surface Temperatures are also indicated at the surface layer with red dots.

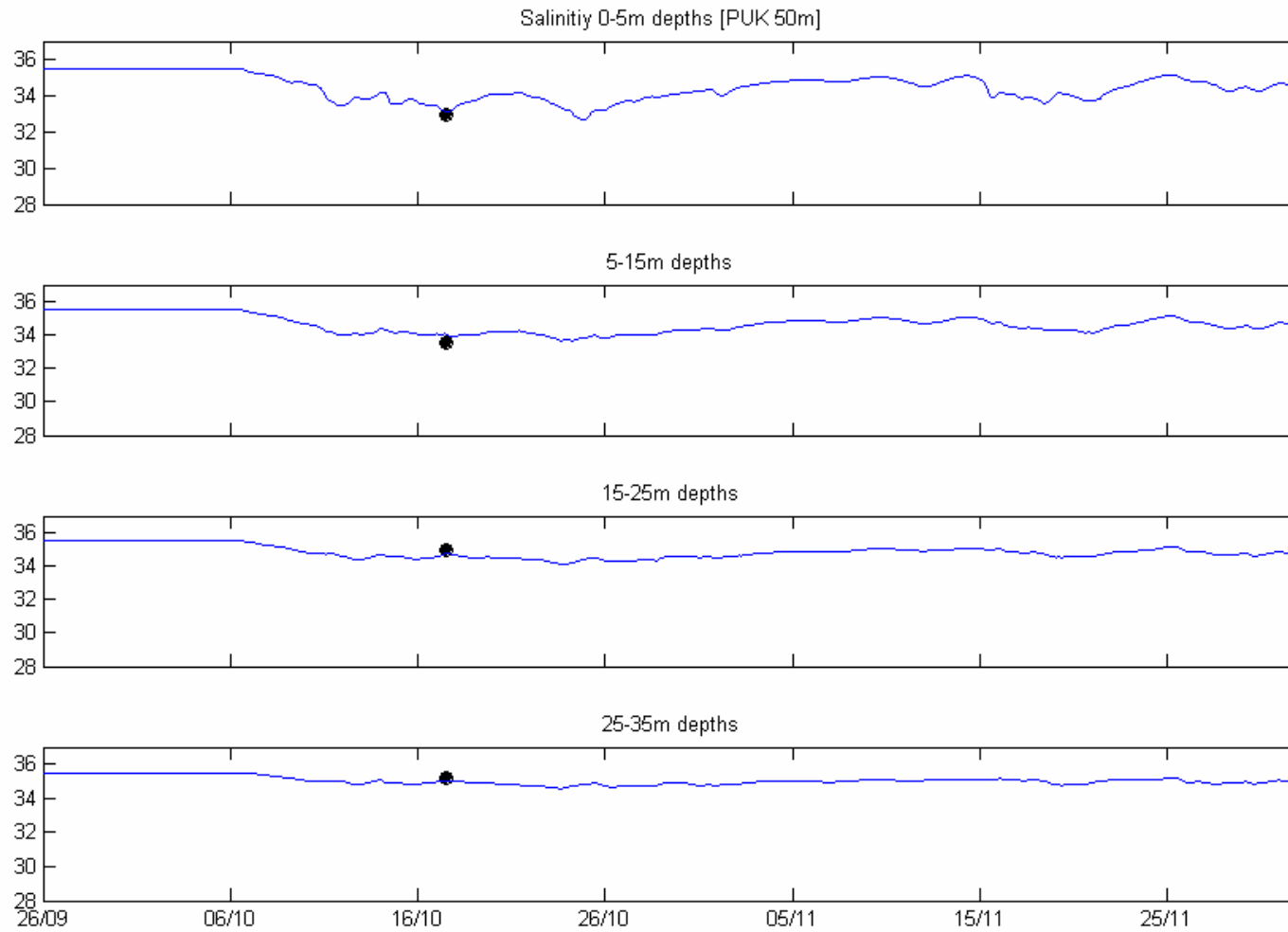


Figure 6.13 – Measured (black dots) and modelled (blue line) salinities at the Pukehina 50m site. Salinities were measured with a Seabird CTD. Note that the constant nature of the modelled salinities for the first ~10 days is due to the ‘cold’ model start and the lag time for the reduced salinity water to reach this site.

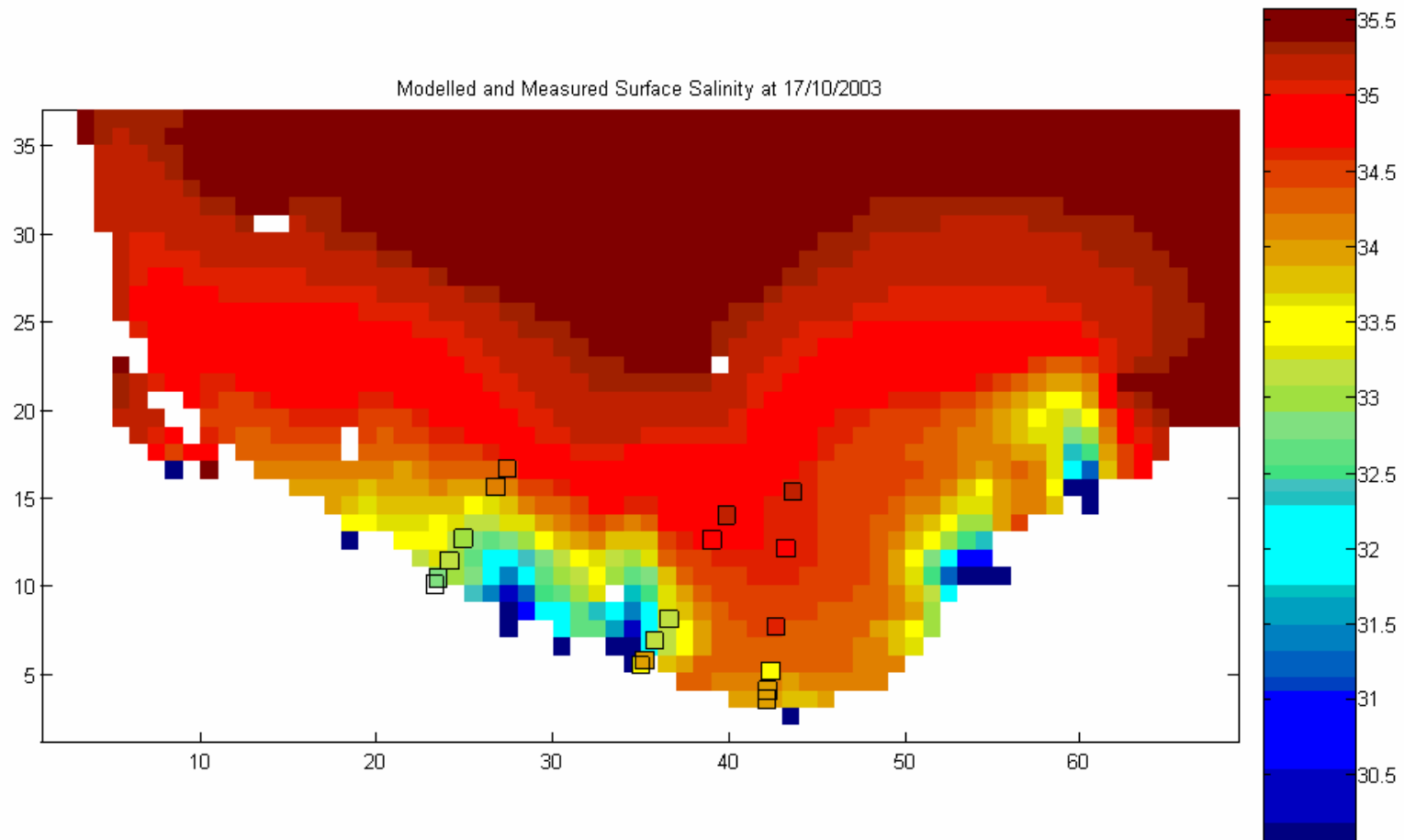


Figure 6.14 – Measured (black squares) and modelled (main grid) surface salinities on 17 October 2003. Note that the general pattern of salinities is reproduced well by the model, with the exception of one ‘spurious’ data point off Opotiki.

7 Conclusions

We conclude that the model is able to reproduce the essential dynamics of Bay of Plenty and can be applied to the determination of the potential environmental effects of the Aquaculture farms. In the next stage, the hydrodynamic model is used to drive the Primary Production model 3DDLIFE, which considers impacts of the farms on the nutrients, phytoplankton and zooplankton in the Bay of Plenty due to mussel feeding.

8 References

- Beamsley, B., Black, K.P., Longdill, P.C., and McComb, P., 2005. *Bay of Plenty Current and Temperature Measurements: Aquaculture Management Areas*. Report for Environment Bay of Plenty, ASR Ltd, P.O. Box 67, Raglan, NZ, 65p.
- Black, K. P. 1989: Numerical simulation of steady and unsteady meso-scale eddies. *Proceedings, 9th Australasian Conference on Coastal and Ocean Engineering* Adelaide, pp. 204-208.
- Black, K.P. 1995: The hydrodynamic model 3DD and support software. *Occasional Report 19, Dept. of Earth Sciences, University of Waikato*, 53 p.
- Black, K .P.; Gay, S.L.: 1987: Eddy formation in unsteady flows. *Journal of Geophysical Research* 92, 9514-9522.
- Black, K.P.; Hatton, D.; Rosenberg, M. 1993: Locally and externally-driven dynamics of a large semi-enclosed bay in southern Australia. *Journal of Coastal Research* 9 (2), 509-538.
- Black, K. P.; Bell R.G.; Oldman J.W.; Carter G.S.; Hume T.M. 2000: Features of 3-dimensional barotropic and baroclinic circulation in the Hauraki Gulf, New Zealand. *N.Z. Journal Marine and Freshwater Research* 34:1-28.
- Black, K.P., Oldman, J., Hume, T. 2005. Dynamics of a 3-dimensional, baroclinic, headland eddy. *New Zealand Journal of Marine and Freshwater Research*. 39 91-120.
- Egbert, G., Bennett, A., Foreman, M., 1994. TOPEX/Poseidon tides estimated using a global inverse model, *J. of Geophys. Res.*, vol99, No C12, pp. 24,821 - 24, 852

- Lamb, K. G. 1994: Numerical simulations of stratified inviscid flow over a smooth obstacle. *Journal of Fluid Mech.* 260, 1-22.
- Leendertse J.J.; Liu, S-K. 1975: Modelling of three dimensional flows in estuaries. 2nd Annual Symposium on Modelling techniques. *Waterways Harbours and Coastal Engineering* (ASCE) pp 625-642.
- Longdill, P.C., Black, K.P., Park, S. and Healy, T.R., 2005. *Bay of Plenty Shelf Water Properties Data Report 2003 – 2004: Aquaculture Management Areas*. Report for Environment Bay of Plenty, ASR Ltd, P.O. Box 67, Raglan, NZ, and the University of Waikato. 35p.
- Middleton, J.F.; Black K.P. 1994: The low frequency circulation in and around Bass Strait: a numerical study. *Continental Shelf Research* 14 (13/14), 1495-1521.
- Perrels, P.A.J.; Karelse, M. 1982: A two-dimensional laterally averaged model for salt intrusion in estuaries. *Delft Hydraulics Laboratory Report No.* 262.
- Sutton, P.J.H., and Roemmich, D., 2001. Ocean temperature climate of north-east New Zealand. *New Zealand Journal of Marine and Freshwater Research* 35, 553-565.
- Wu, J. 1982: Wind stress coefficients over sea surface from sea breeze to hurricane. *Journal Geophysical Research* 87 : 9704–9706.
- Young, I.R.; Black, K.P.; Heron, M. L. 1994: Circulation in the ribbon Reef Region of the Great Barrier Reef. *Continental Shelf Research* 14 (2/3), 117-142.